PRECIPITATION NOISE MEASUREMENTS ON JET TYPE AIRCRAFT

ROBERT WALTER SLEZAK

Artisan Gold Lettering & Smith Bindery

593 - 15th Street   Oakland, Calif.   GLencourt 1-9827

DIRECTIONS FOR BINDING

BIND IN (CIRCLE ONE)	SHELF LETTERING ON BACK TO BE EXACTLY AS PRINTED HERE.
BUCKRAM COLOR NO. 8854	SLEZAK
FABRIKOID COLOR	1954
LEATHER COLOR	Thesis S571

OTHER INSTRUCTIONS

Letter on the front cover:

PRECIPITATION NOISE MEASUREMENTS
ON JET TYPE AIRCRAFT

ROBERT WALTER SLEZAK

PRECIPITATION NOISE MEASUREMENTS
ON JET TYPE AIRCRAFT

by

Robert Walter Slezak

Lieutenant, United States Navy

Submitted in partial fulfillment
of the requirements
for
CERTIFICATE OF COMPLETION

United States Naval Postgraduate School
Monterey, California

1954

This work is accepted as fulfilling

the thesis requirements for a

CERTIFICATE OF COMPLETION

from the

United States Naval Postgraduate School

PREFACE

Precipitation static has long been recognized as a particularly serious problem in aviation radio navigation and communication systems. Many investigations as to its causes and nature have been made[8, 11, 20] with successful progress, especially during the past fifteen years. Static free navigational systems (VOR Omni-range), for short ranges, and line of sight communications systems (VHF-UHF), are now standard equipment on all aircraft, although it must be pointed out that these solutions involve a sort of strategic retreat, that is, a shift to higher frequency levels where the precipitation static energy content is of a lesser value. Also the investigations that were made all utilized propeller driven aircraft for their test vehicles and although projects were earmarked to include jet type of aircraft, none, to the author's knowledge, were ever reported on.

The problem that is the subject of this thesis was essentially to design a device to measure the relative noise power or voltage due to corona discharge, at certain specified locations in the frequency spectrum, and be carried aboard jet type aircraft. This is a bit of a swift explanation but a detailed account will be given later.

Also an attempt is made to correlate information regarding some of the statistical aspects of noise analysis and although it is not a completely rigid treatment, it describes in a condensed manner, a description of noise signals and their effects on electronics circuits.

The author would like to express great appreciation to Messrs. H. P. Blanchard and Maurice Mills of the Stanford Research Institute for

their infinite patience and guidance, and to Professors Robert Bauer and Robert Kahal for encouragement and interest.

TABLE OF CONTENTS

Page

Certificate of Approval i

Preface ii

Table of Contents iv

List of Illustrations v

Chapter I - Introduction 1

1. History and General Considerations of the Problem 1
2. The Projected Method of Solution 8
3. A Development of Mathematical Description of Random Noise 10
4. Previous Statistical Noise Measurements 16

Chapter II - Description of Designed Measuring Devices 18

1. System I - The Mean Square Noise Meter 20
2. System II - Navigational Device Simulator & Recorder . . 29
3. Operation 43

Chapter III - Results and Conclusions 44

1. Results 44
2. Conclusions 48

Appendix I 52

Appendix II 55

Bibliography 59

LIST OF ILLUSTRATIONS

Figure Page

1. Simplified Diagram of Navigational System . . . 4

2. Idealized Waveforms 6

3. Graph of i(t) versus Time 11

4. Graph of i(t) versus Time for the Interval 2T . 11

5. Corona Pulse Generator 45

6. Plot of Noise Power Spectrum 50

I-0 Block Diagram of System I 23

I-1 R-F Tuning 24

I-2 Log Amplifier 25

I-3 Square Law Circuit 26

I-4 Miller Integrator and Detector 27

I-5 Meter Coupling Circuit 28

II-0 Block Diagram of System II 35

II-1 Input Circuit and Tuned Amplifier 36

II-2 Log Amplifier 37

II-3 126 kc Oscillator and Phase Shift Network . . . 38

II-4 126 kc Amplifier, Gate and Miller Integrator . 39

II-5 400 cycle Oscillator and Amplifiers 40

II-6 400 cycle Chopper and Amplification Stages . . 41

II-7 Detector and Recorder Circuit 42

III Mean Noise Level Recording of Aircraft in Flight 46

IV Noise Level Recording of Cumulus Cloud Formation 47

Chapter I

INTRODUCTION

1. History and General Considerations of the Problem

Precipitation static may be described as radio interference caused by corona discharge. It is sometimes labled as, 'Poisson noise', is technically named, 'impulse noise', and is statistically described as, 'nearly normal random noise'. It is but a single type of the many kinds of noise that have been studied, analyzed and catalogued, although it does have the dubious distinction of being the number one culprit of aviation navigational and communications systems.

The first analysis and explanation of precipitation static was that charged particles, created by the turbulence and charged energy of thunder clouds, generated static when striking the antenna. No attempts were made to alleviate these effects for many years until the introduotion of the shielded loop antenna in 1934. It was assumed that since particles did not strike the antenna proper, static would be reduced. However, this assumption was not substantiated in practice because it was found that in actual air operation, severe static easily disabled the system.

In 1939 after more investigation, a new theory [11] assigned the main cause of precipitation static in aircraft to that of corona discharge. Later the concentrated effort of the Army-Navy Precipitation Static Project [8] verified this theory which resulted in the subsequent changes to air-frame construction and airborne electronic equipment that are in standard practice today.

With the increased use of jet and rocket propulsion in supersonic

aircraft and guided missiles, it was erroneously assumed that the determinental effects due to precipitation static would be of no consequence, since in this type of craft, a natural discharging process due to the thermal ionization of the exhaust gases, should efficiently transfer free charge to the atmosphere. This is partially accomplished because a complete recombination of the ions produced in burning the fuel has not as yet taken place, thus the electric field of the aircraft will capture those ions of opposite sign while simultaneously repelling those of the same sign.[8]

In a recent report by R. L. Tanner,[20] it was shown that the strength of the noise signals due to corona discharge is directly related to the dipole moment of the discharge current. The dipole moment is proportional to the product of the current flow and the distance over which it takes place. Thus in any supersonic aircraft which strikes ice crystals (cumulo-cirrus type clouds), or heavy turbulence (cumulo-nimbus type clouds), or the layers of ionized air located at extremely high altitudes, a static charge builds up in the vicinity of plastic antenna housings, canopies and control surfaces. It is here that one is faced with a new type phenomenon that is based on a very old principle: that substances of high dielectric constant acquire a positive charge when rubbed with substances of lower dielectric constant. This is called triboelectric charging, and can be visualized as a scrapping off of the electrons by the airstream. Naturally this charging eventually culminates in a corona type discharge at many points close to the outer perimeter of plastic housings and the dipole moment of the current discharge acts as an efficient antenna to couple this electrical noise into the receiver input circuits.

The problem specifically, is to determine the average noise power or

the average voltage produced by this static, recorded for a period of time equal to the flight duration of the aircraft. This system must duplicate an actual navigational system's characteristics with respect to bandwidth, resonant frequency, servo system time constants and antenna matching stage.

The actual navigational system can be represented in general by the diagram in Figure 1.

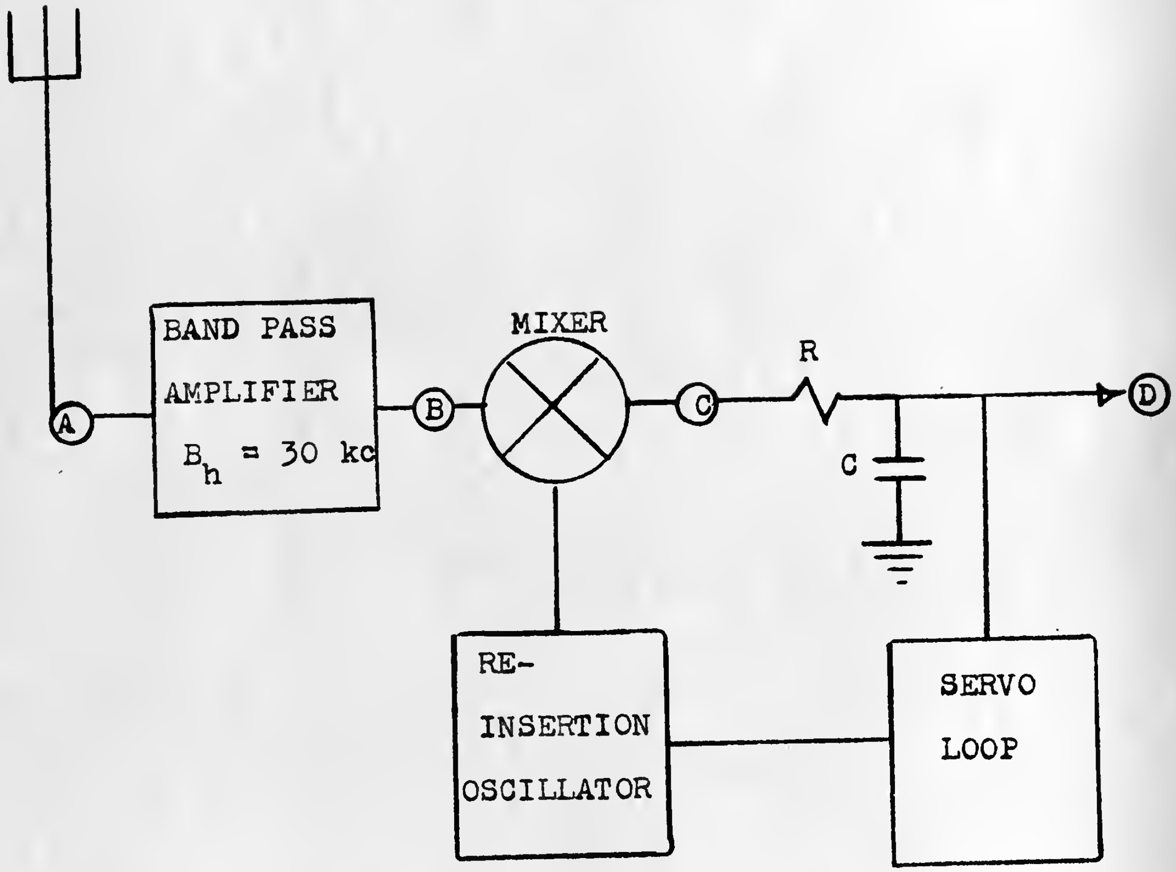

TIME CONSTANT

RC = 100 seconds

FIGURE 1

Simplified Diagram of Navigational System

To illustrate:

If the incoming waveform is sinusoidal in nature, then the output of the mixture will be the sum and difference terms of the original inputs. This is applied to the integrator which acts to average only the difference terms since it is a low pass filter. The output will then be a very slowly varying voltage and the subsequent error signals will also be very small in magnitude.

Where precipitation static is present the waveforms (idealized) might take the form of those shown in Figure 2. Since power is proportional to the voltage applied to the servo system, the disturbance to the system is related to all the input noise pulses integrated over a period of time equal to the time constant of the system, and can be written as

$$\frac{1}{T}\int_0^T E\,dt = \text{Phase Disturbance in System}$$

The error signal to the reinsertion oscillator will then be proportional to the input average noise power so that periods of heavy static would precede large error signals.

The system that was designed and constructed duplicating the above characteristics is now being operationally used to record the average noise power over periods of ten to twelve hours. These results are later compared to the navigational errors plotted separately by the navigator to see what relative values of average noise power cause the maximum errors in the system.

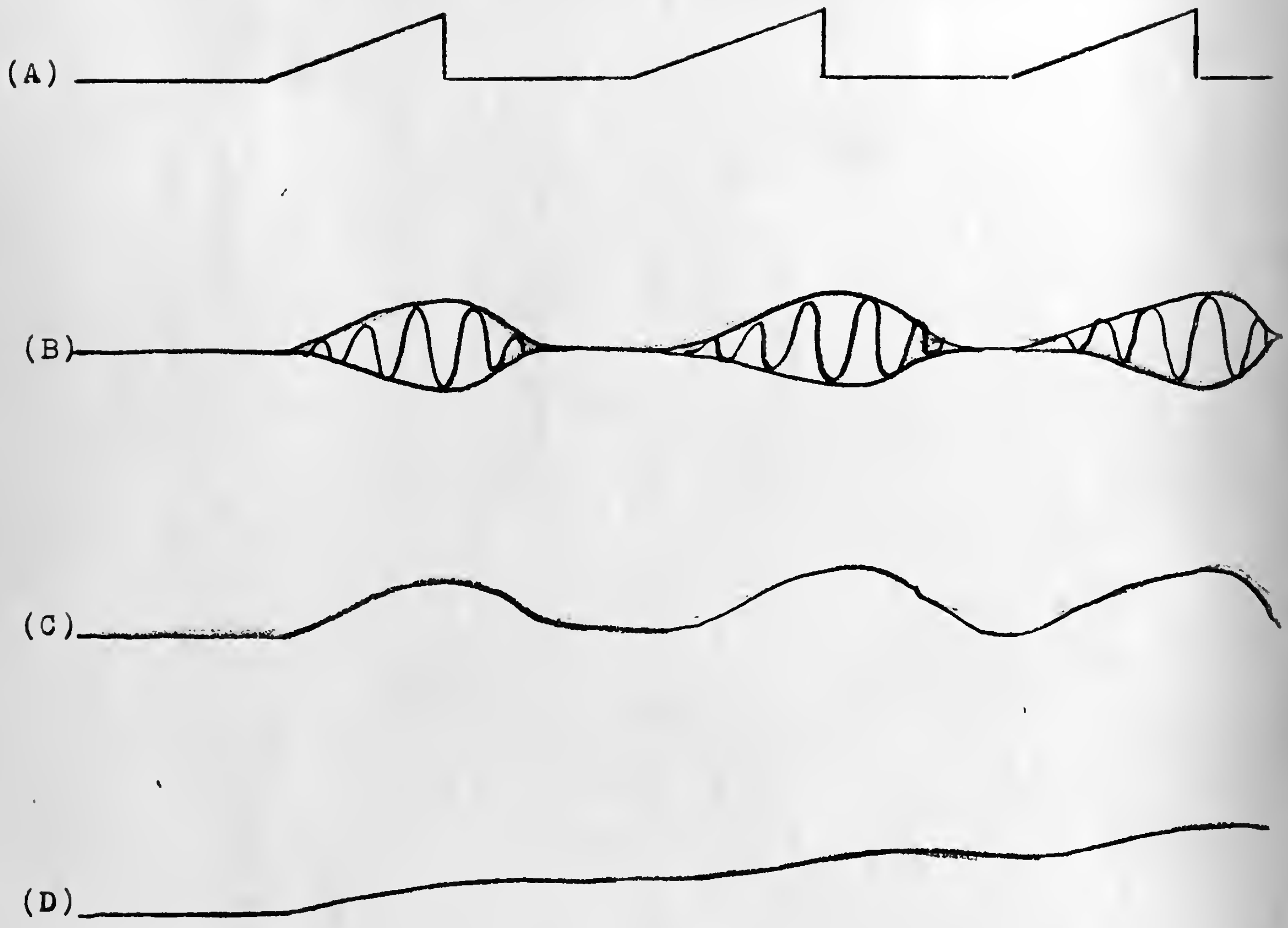

FIGURE 2

Idealized Waveforms

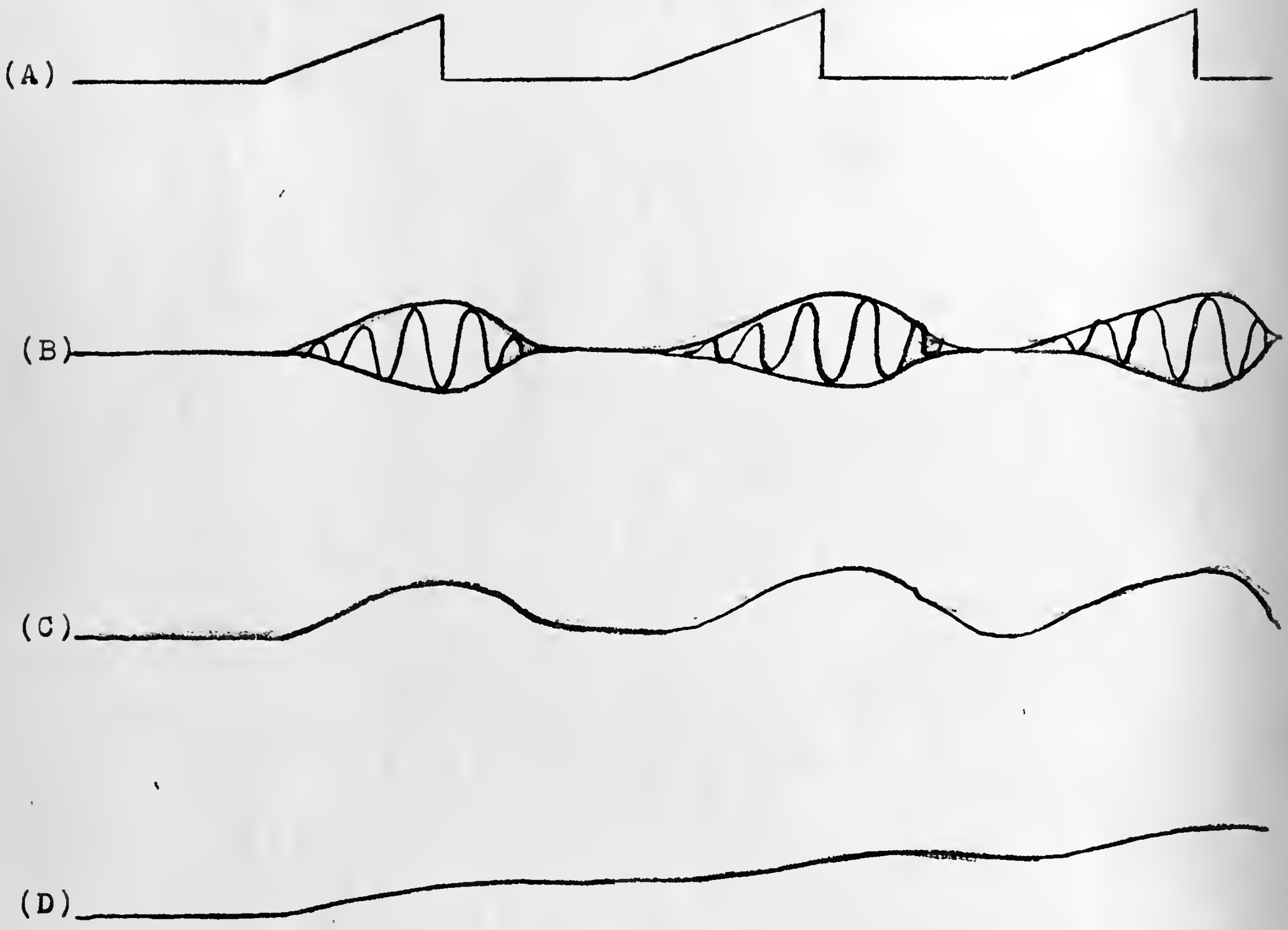

FIGURE 2

Idealized Waveforms

A second system to measure the average noise power at specific frequencies is also described in Chapter III with some data which shows results of actual flights made using the system.

2. The Projected Method of Solution:

A study of the available systems for measuring noise due to atmospheric sources and corona discharge indicates a common tendency to make the majority of measurements using an electric field intensity meter, or circuits of some such similar nature. The results are then interpreted using a graphical portrayal of corona discharge current as a function of electrical field intensity. In this problem it is desired to measure the energy components of the noise at a specified frequency and known bandwidth, therefore a relationship with respect to time must be set up to measure this noise power. But the instantaneous noise voltage induced in the antenna cannot be considered as a regular function of time, for if it were, both amplitude and phase relationships would have to be known for one complete period. Since it cannot, the problem is one that is statistical in nature.

Statistics may be succinctly defined as the science of reduction and analysis of data. Its application to the problems associated with communication processes can be mainly attributed to N. Wiener,[22] who was one of the foremost contributors during the development years of statistical prediction theory, particularly concerning stationary random time functions, a random time function being defined as a function which does not follow any specific law of variation and therefore is not precisely predictable. The type of noise being investigated in this paper falls into this category for it consists of a superposition of impulses occurring at random times with overlapping individual pulses. It is sometime referred to as Poisson noise because the Poisson distribution (Appendix I) is used to describe its statistical structure. In statistical applications the Poisson Distribution often appears when concerned with the number of

occurrances of a certain event for a very large number of observations, where probability for the event to occur in each observation is very small.[3,5] It is for this reason that it is sometimes called the "small probability law". For the case of very high density Poisson noise, that is, when the number of elementary random impulses is large, and their mean duration is not too brief, a heavy overlapping occurs and the result is nearly normal random noise. This, according to Middleton[17] can be considered to have a normal distribution with negligible correction terms, and the shape of the pulse is unimportant. (Appendix I)

It is plausible to assume that the corona discharge that takes place will have the characteristics of high density Poisson noise, for when the same navigational system was operated in slower propeller driven types of aircraft, the system suffered erratic operation (intolerable errors), only when thunder storms set up exceedingly heavy corona conditions. Also, the system operated normally under conditions of moderate corona indicating that the low density types can be ignored.

For the case of the jet aircraft, the corona discharge intensity would be mainly a function of speed and since the latter is usually close to maximum designed speed, the intensity will always be close to maximum, with corona discharge pulses occurring at all of the places where plastic surfaces are exposed to the airstream. The mathematical theory to describe this phenomena is covered below and is closely allied to the more familiar treatment of fluctuation noise.

3. A development of Mathematical Description of Random Noise.

Consider a plane-electrode diode for the emission limited case. A graph showing the current versus time for a single electron leaving the point of zero potential ($t = 0$), and arriving at the point of highest potential ($t = t_n$), is shown in Figure 3. When a constant potential is assumed over a time interval 2T, and a pulse having the shape of that shown in Figure 3, takes place for each electron crossing, a plot of the current I(t) versus time for the interval 2T is shown in Figure 4.

Assume that N electrons are emitted during the interval indicated. Then I(t) is the sum of the individual current pulses

$$I(t) = \sum_{N=1,2,3\cdots}^{N} i(t - t_n) \qquad 1\text{-}1$$

and the time average is

$$\bar{I}(t) = \lim_{T \to \infty} \frac{1}{2T} \int_{-T}^{T} I(t)\, dt = \lim_{T \to \infty} \frac{1}{2T} \int_{-\infty}^{\infty} I(t)\, dt \qquad 1\text{-}2$$

substituting

$$\bar{I}(t) = \lim_{T \to \infty} \frac{1}{2T} \sum_{N=1,2,3\cdots}^{N} \cdot \int_{-\infty}^{\infty} i(t - t_n)\, dt \qquad 1\text{-}3$$

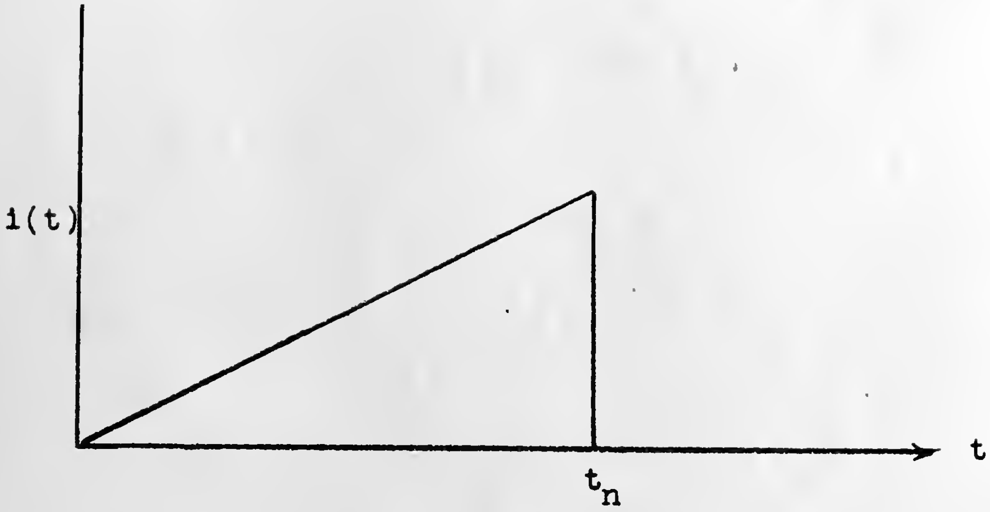

FIGURE 3

Graph of i(t) versus Time

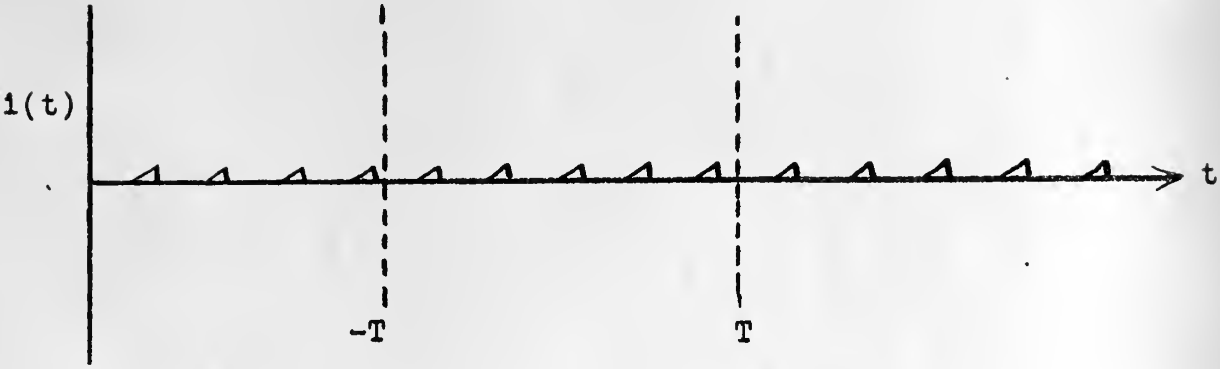

FIGURE 4

Graph of i(t) versus Time Showing the Interval 2T

Now consider the electron stream to be made up of a great number of electrons whose fluctuations are considered to be random.[19] A count of electrons arriving at the plate in the interval 2T is N. Repeating this count for a total number of M times gives a value for the average number of electrons per second as

$$V = \lim_{M \to \infty} \frac{N_1 + N_2 + N_3 + \cdots + N_M}{M(2T)} \tag{1-4}$$

As M is increased and T held constant, some of the N's will have the same value, thus the number of N's of a particular value will increase as M is further increased. The probability of getting N electrons for some particular trial is defined as

$$p(N) = \lim_{M \to \infty} \frac{\text{Number of trials giving N electrons}}{M} \tag{1-5}$$

Since p(N) also depends on T it can be assumed that the randomness of the electron stream is such that the probability that an electron will arrive at the anode in the interval $(t, \quad t + \Delta t)$ is

$v\,\Delta t$ where Δt is such that $v\Delta t \ll 1$, and that this probability is independent of what happened before time t or what will happen after time $t+\Delta t$. For a very large number of trials this is a description of the Poisson distribution and is expressed as

$$p(N) = \frac{(2vT)^N}{N!}\, e^{-2vT} \qquad 1\text{-}6$$

Thus a large number, M, of intervals of length 2T having exactly N arrivals will be to a first approximation $Mp(N)$. For a fixed value of t, equation 1-3 may be written

$$\overline{I_N(t)} = \sum_{N=1,2,\dots}^{N} \frac{1}{2T}\int_{-T}^{T} i(t-t_n)\,dt_N \qquad 1\text{-}7$$

and for $\Delta < t < T-\Delta$ it effectively becomes

$$\overline{I_N(t)} = \frac{N}{T}\int_{-\infty}^{\infty} i(t)\,dt \qquad 1\text{-}8$$

It is now possible to write the average I(t) over all of the M intervals instead of only over those having N arrivals, so as M

$$\overline{I(t)} = \sum_{N=0}^{\infty} \overline{p(N)\, I_N(t)} \qquad 1\text{-}9$$

$$= \sum_{N=0}^{\infty} \frac{N}{2T}\,\frac{(2vT)^N}{N!}\, e^{-2vT}\int_{-\infty}^{\infty} i(t)\,dt \qquad 1\text{-}10$$

$$= v\int_{-\infty}^{\infty} I(t)\,dt \qquad 1\text{-}11$$

Campbell's theorem[19] states that the mean square value of the fluctuation about the average is

$$\overline{(I(t) - \overline{I(t)})^2} = v \int_{-\infty}^{\infty} i^2(t)\, dt \tag{1-12}$$

$$= I^2(t) - \overline{2I(t)\,\overline{I(t)}} - \overline{I(t)^2} \tag{1-13}$$

Since

$$I_N^2\,(t) = \sum_{n=1}^{N} \sum_{m=1}^{N} i(t - t_n)\, i(t - t_m) \tag{1-14}$$

Averaged over all values of t_1, t_2, t_3, ... t_N, with t held fixed

$$\overline{I_N^2(t)} = \sum_{n=1}^{N} \sum_{m=1}^{N} \int_{-T}^{T} \frac{dt_1}{2T} \cdots \int_{-T}^{T} \frac{dt_N}{2T}\, i(t-t_n)\, i(t-t_m) \tag{1-15}$$

The multiple integral has two different values, so when n = m

$$\int_{-T}^{T} i^2(t-t_n) \frac{dt_n}{2T} \tag{1-16}$$

and for n ≠ m its value is

$$\int_{-T}^{T} i(t-t_n) \frac{dt_n}{2T} \int_{-T}^{T} i(t-t_m) \frac{dt_m}{2T} \tag{1-17}$$

Counting up the number of terms in the double sum shows that there are N of them having the first value and $N^2 - N$ having the second value.

For $-T+\Delta < t < T-\Delta$

$$I_N^2(t) = \frac{N}{2T}\int_{-\infty}^{\infty} i^2(t)\,dt + \frac{N(N-1)}{N^2}\left[\int_{-\infty}^{\infty} i(t)\,dt\right]^2 \qquad \text{1-18}$$

Averaging over all the intervals instead of only those having N arrivals, the final form can be written as

$$\overline{I^2(t)} = \sum_{N=0}^{\infty} P(N)\,\overline{I_N^2(t)} \qquad \text{1-19}$$

$$= V\int_{-\infty}^{\infty} i^2(t)\,dt + \overline{I(t)}^2 \qquad \text{1-20}$$

where the summation with respect to N is performed as in (1-11) and after the summation, the value (1-11) for $\overline{I(t)}$ is used.

The relationship of the above development to the problem can be shown for a small increment of surface area located at one of the points where the metallic airframe and plastic housing are adjacent.

By equation 1-1 the individual current pulses can be described for a single element, and when all of the points are taken into consideration, plus all of the locations where plastic housings are adjacent to metallic airframe, equation 1-20 expresses the total average squared current. (Appendix I)

4. Previous Statistical Noise Measurements

Some investigation of other statistical approaches to the measurement of noise was made before any design considerations were conceived.

In their article, "A Statistical Approach to the Measurement of Atmospheric Noise" by R. S. Hoff and R. C. Johnson,[10] it states in part,"... that atmospheric noise, causing noise voltage to be induced into a receiving antenna...the envelope of this noise voltage after being amplified by the receiver stages and further modified by limiting and other nonlinear processes, is an irregular function of time or time series Y(t), and may be treated by statistical processes." Also, Landon[14] has shown that the distribution of noise voltage when passed through a narrow band filter is normal (Gaussian),(Appendix I) that is, the fluctuation noise output of a band pass amplifier has a distribution of voltage versus time which follows the normal error law. The method used is similar to that used by Lord Rayleigh[18] in determining the probable distribution with time of the instantaneous amplitude of a large number of sine waves, all with equal amplitudes and random relative phases. From Knudzton's report[12], "... that the narrow band noise has the character of an amplitude and frequency modulated wave for the ideal rectangular band pass filter, where the average period of the envelope is a linear function of the bandwidth only."

Thus it is possible to list the conditions that will effect the design characteristics of the device to examine the properties of the precipitation noise.

(1) If a quantitative value of the noise power is desired, a narrow band pass filter of approximately 3 kc must be used since the center frequency is 126 kc. (See Appendix II)

(2) The device must simulate a navigational system which has the fol-

lowing characteristics:

(a) Bandwidth 30 kc

(b) Resonant Frequency 126 kc

(c) Servo time constant response - 100 seconds

(3) Ideally considered, the noise has a white spectrum. This of course is not true, but is permissible for this problem since Plank's radiation formula indicates that the thermal noise energy is down 1/e of its maximum value of KT at about 10^7 mc.[5]

To satisfactorily solve this dilemma of having two bandwidths it would be necessary to have two distinct systems; the first to measure a quantitative value of the noise, and the second to ride next to the navigational system recording the relative noise input level for a specified navigational track. It was decided to use the latter system to study the effects peak disturbance periods as a function of navigational error and to use the first system to set up a method to investigate the power spectrum of high density precipitation static by measuring the average power level across the band in small increments of frequency.

Chapter II

Description of Designed Measuring Devices

1. SYSTEM I - MEAN SQUARE NOISE METER

As shown in Appendix II, it is possible to represent the output of a narrow band filter by

$$e(t) = e_{\cos}(t) \cos w_m t + e_{\sin}(t) \sin w_m t$$

Using a very narrow band pass amplifier as the input stage, the mean value of the output noise voltage can be found by integrating the voltage over a long period of time. This integrator has an output which is made up of a component that increases linearly with time, plus some variation due to the input a-c components which are smoothed out after sufficient elapsed time. It is specifically desired to record the mean square value of the noise voltage ($\overline{e}^2$), by constructing a device which will square the input and then integrate the low frequency (difference terms) components over a long period of time. The advantages are:

(a) The recorded measurements are proportional to energy.

(b) From the basic premise, that the noise has a normal distribution, it must then consist of a uniform spectrum of Spectral Density N_o volts^2 /cps at all frequencies other than zero, and have a true mean value ($\overline{e}$)volts, it is necessary to continue the integration process for a length of time

$$T = (2 \times 10^4 \ N_o) / P^2 \ \overline{e}^{\,2} \text{sec}$$

in order to insure a 95% certainty that the measured value lies within P percent of the true mean.[1]

Frequency Analysis of the Square Law Circuit: The current of a diode may be represented by the infinite series

$$i_p = c_1 e + c_2 e^2 + c_3 e^3 + \dots\dots\dots\dots + c_n e^n$$

in which the constants c_n may be determined as are the coefficients in a Taylor series.

Since the diodes are operated in a region where the dynamic characteristic is not a straight line, let it be assumed that the first two terms accurately represent the portion of the characteristic used. Thus

$$i_p = c_1 e + c_2 e^2$$

Substituting equation III-7: Appendix II

$$i_p = c_1 (e_c(t) \cos w_m t + e_s(t) \sin w_m t)$$
$$+ c_2 (e_c(t) \cos w_m t + e_s(t) \sin w_m t)^2$$

The only terms of interest are those containing difference terms since the integrator is essentially a low pass filter, therefore in this case it is

$$2 c_2 e_c(t) e_s(t) \sin w_m t \cos w_m t$$

By trigonometric identities this is equal to

$$2 c_2 e_c(t) e_s(t) \left[\sin (w_m - w_o) t + \cos w_m t \sin w_o t \right]$$

Thus the presence of the difference terms allows the use of a large time constant in the integrator circuit to average the input low frequency terms.

Description of Circuits in System I

Figure I-0 Block Diagram of the System

Figure I-1 Narrow Band Pass Amplifier - Essentially a tuned grid, tuned plate tank, measured to be 3kc wide at half power points, with center frequency at 126 kc, and tunable over a 30 kc band.

Figure I-2 - Logarithmic Amplifier - The amplifier is an instantaneous linear amplifier designed to obtain a large linear range. A feedback loop from the Miller integrator circuit which has a time constant of 100 seconds causes a compressing effect to the input signal. This allows examination of signals whose magnitude may vary from 10 micro-volts to 10^4 micro-volts. The variable gain is calibrated to give approximately 10 db gain for - 6 volts of avc and 70 db gain for - 1 volt avc.

Figure I-3 Square Law Circuit - This circuit was originally designed using the relation

$$E_o = k E_i^2$$

where E_o is the output voltage and E_i^2 is the input voltage of the circuit. Knowing the desired avc characteristic and the time constant of the Miller integrator it is possible to approximate the value of k. This was accomplished by plotting several curves using values close to the approximated value of k, constructing a circuit with variable resistors and adjustable bias levels, empirically determining the component values after the input and output values 'fit' the desired curve.

Figure 1-4 Detector and Miller Integrator - The detector is a peak reading device with a time constant determined by the center frequency

$$\text{T C detector} = 1/1.26 \times 10^5 = 8 \text{ micro-seconds}$$

The basic principle of the Miller integrator in this system is the operation of averaging. It is performed by passing the general input through a low pass filter (integrator), thus the contributions to the output will be made only by those terms which have frequencies which fall within the range of the filter. In this problem the observation interval is fixed at 100 seconds, so thus the output, M(T), of the averaging filter may be related to its input by means of the convolution integral involving the filter's impulse response and weighting function, h(t),

$$M(T) = \int_0^T h(t) \quad E \ (T - t) \, dt$$

where T is the duration of the observation interval.

From "Statistical Errors in Measurements"[4], Table I; the effective bandwidth, B_n and the weighting function, h(t), are given for an integrator as

$$h(t) = 1/T = 0.01 \qquad \text{where } 0 > t > T$$

$$B_h = 1/2T = 0.005$$

The input will be the difference term

$$E_d(t) = 2 \, c_2 \, e_c(t) \, e_s(t) \sin (w_m - w_o)t$$

for

$$0 < w < 0.01$$

Simplifying M(T)

$$M(t) = \int_0^t h(\tau) \ E(t - \tau) d\tau$$

$$\mathcal{L} M = \mathcal{L} h \ \mathcal{L} E$$

$$= \frac{h}{s} \mathcal{L} E$$

$$\mathcal{L} M = h \, \mathcal{L} \int_0^t E$$

$$M = h \int_0^t E + \text{constant}$$

$$M(T) = 0.01 \int_0^T E_c(t) \, dt + \text{Constant}$$

$$M(T) = 0.01 \int_0^{100} 2 C_2 \, e_c(t) \, e_s(t) \sin (W_m - W_0) t$$

$$+ \text{constant}$$

where :

$$0 < W < 0.01$$

The above represents the output of the averaging filter for an observation interval of 100 seconds.

Figure I-5 Meter Coupling Circuit - This circuit uses an Esterline Angus type recorder, Model AW. The meter movement is a 1 ma type.

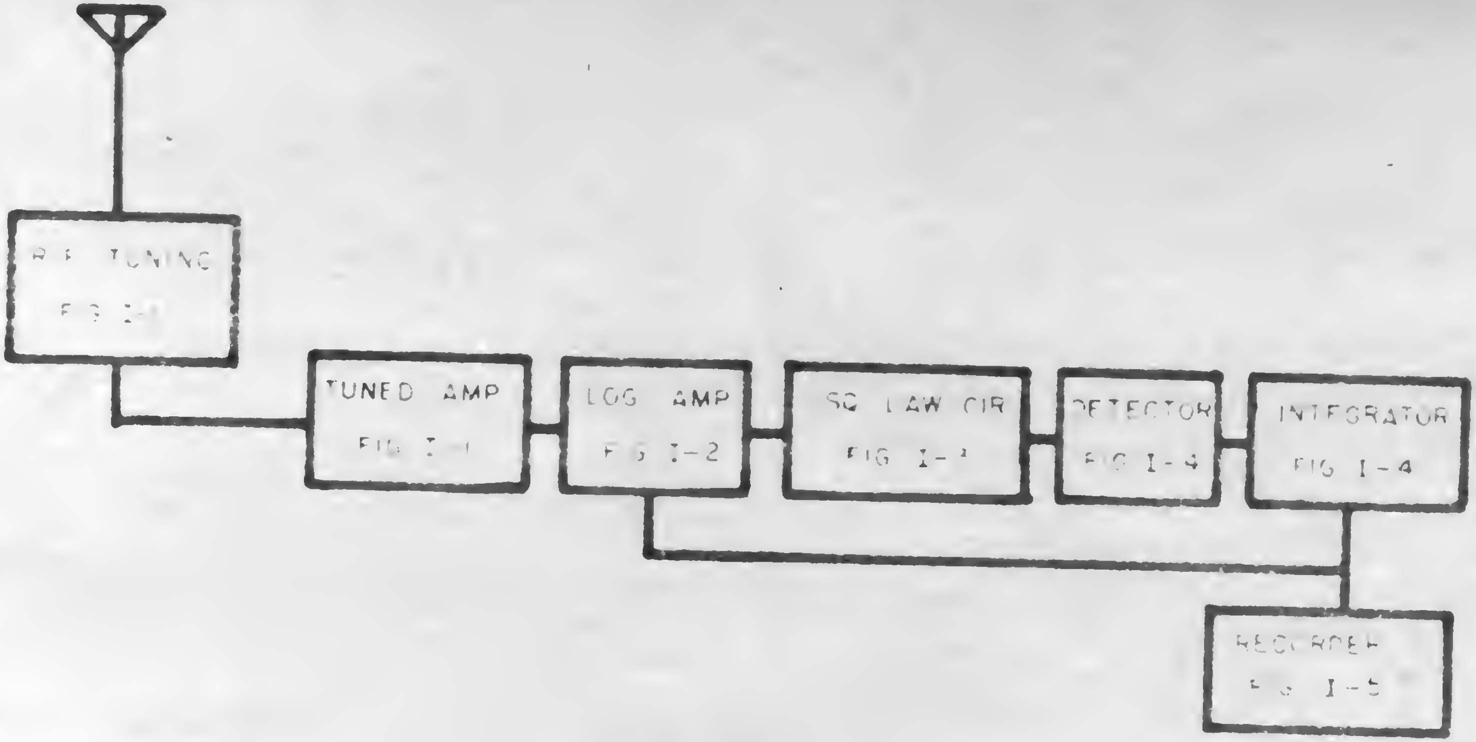

FIG I-6

BLOCK DIAGRAM

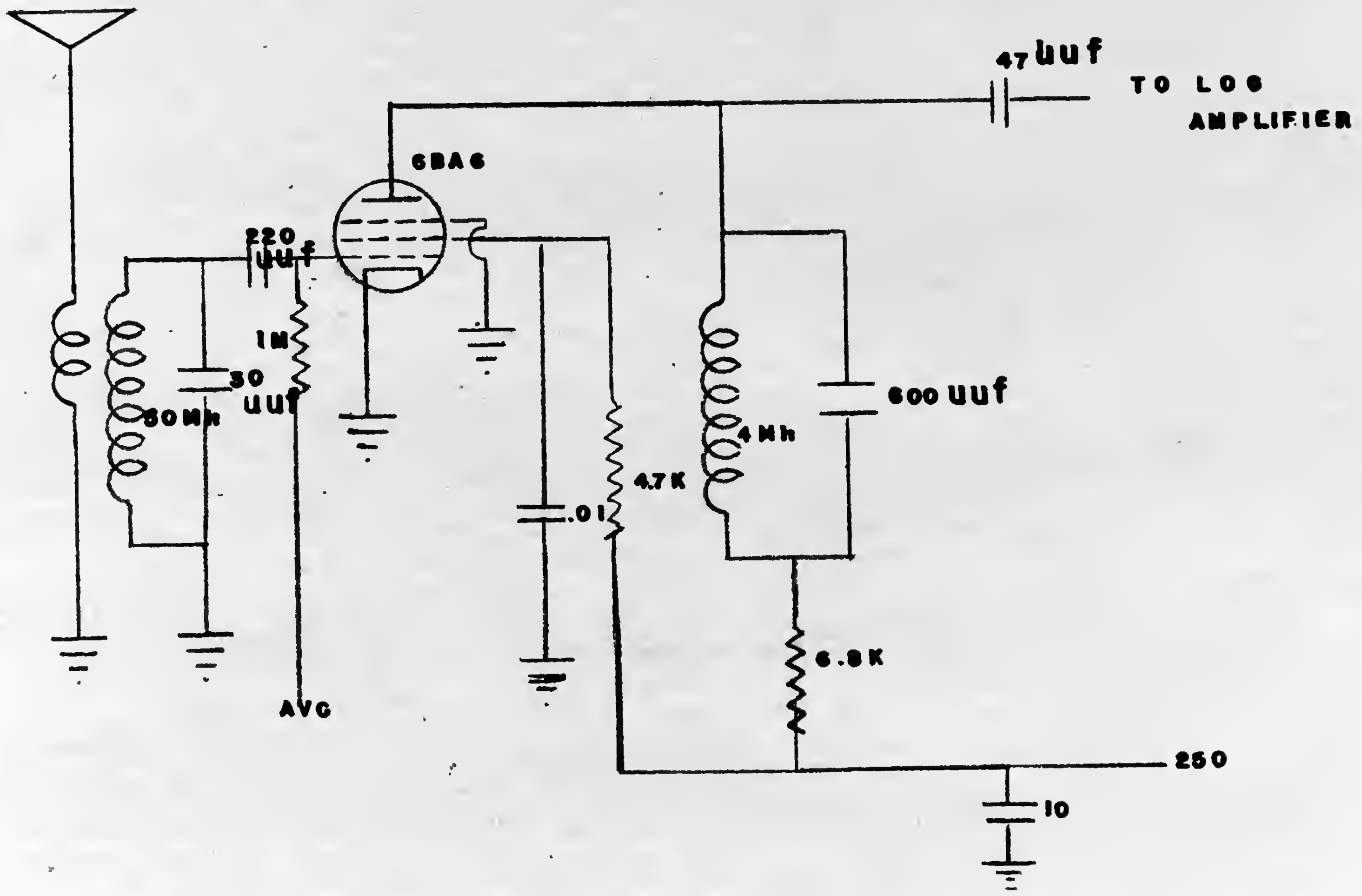

RF TUNING

FIG. II-1

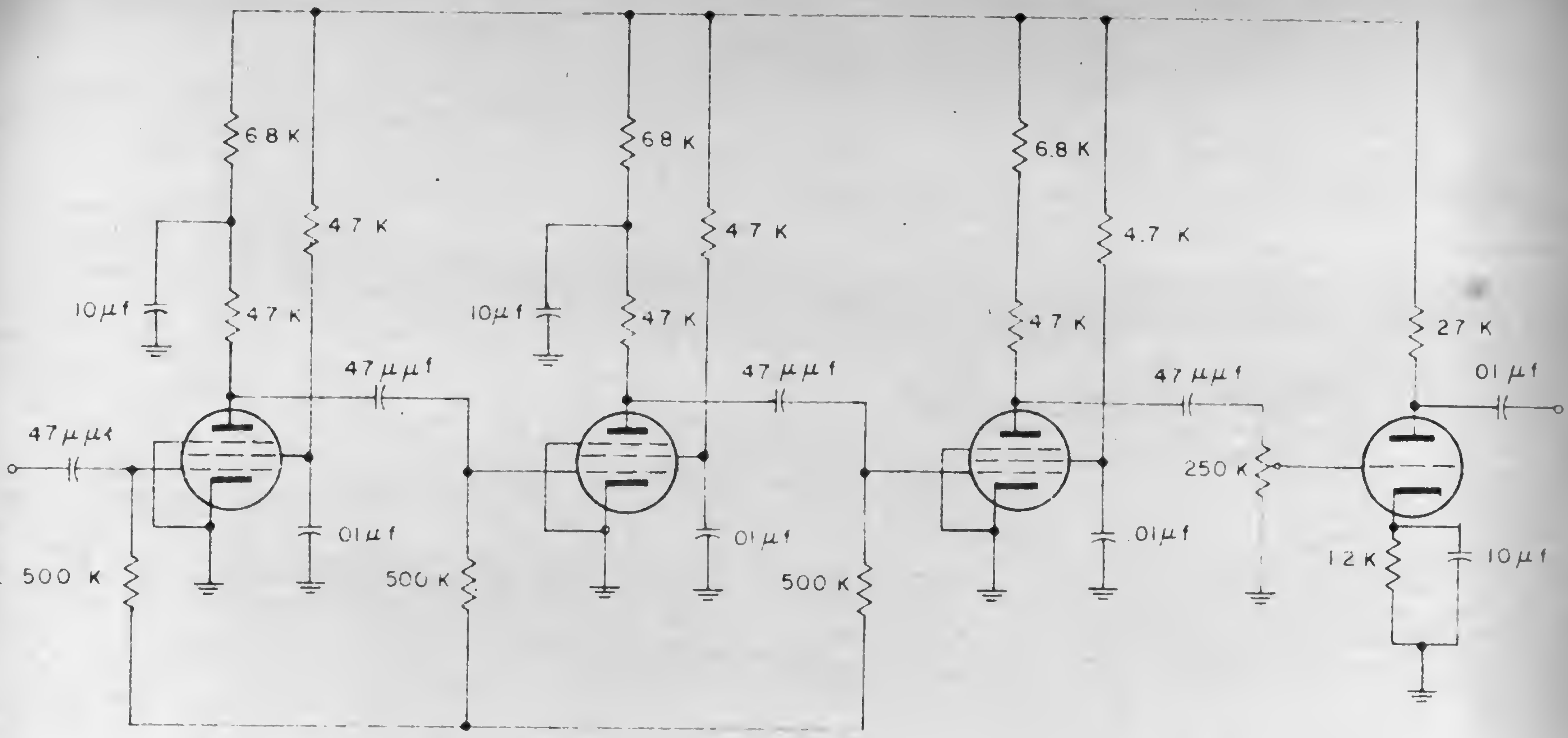

FIG. II-2

LOG AMPLIFIER

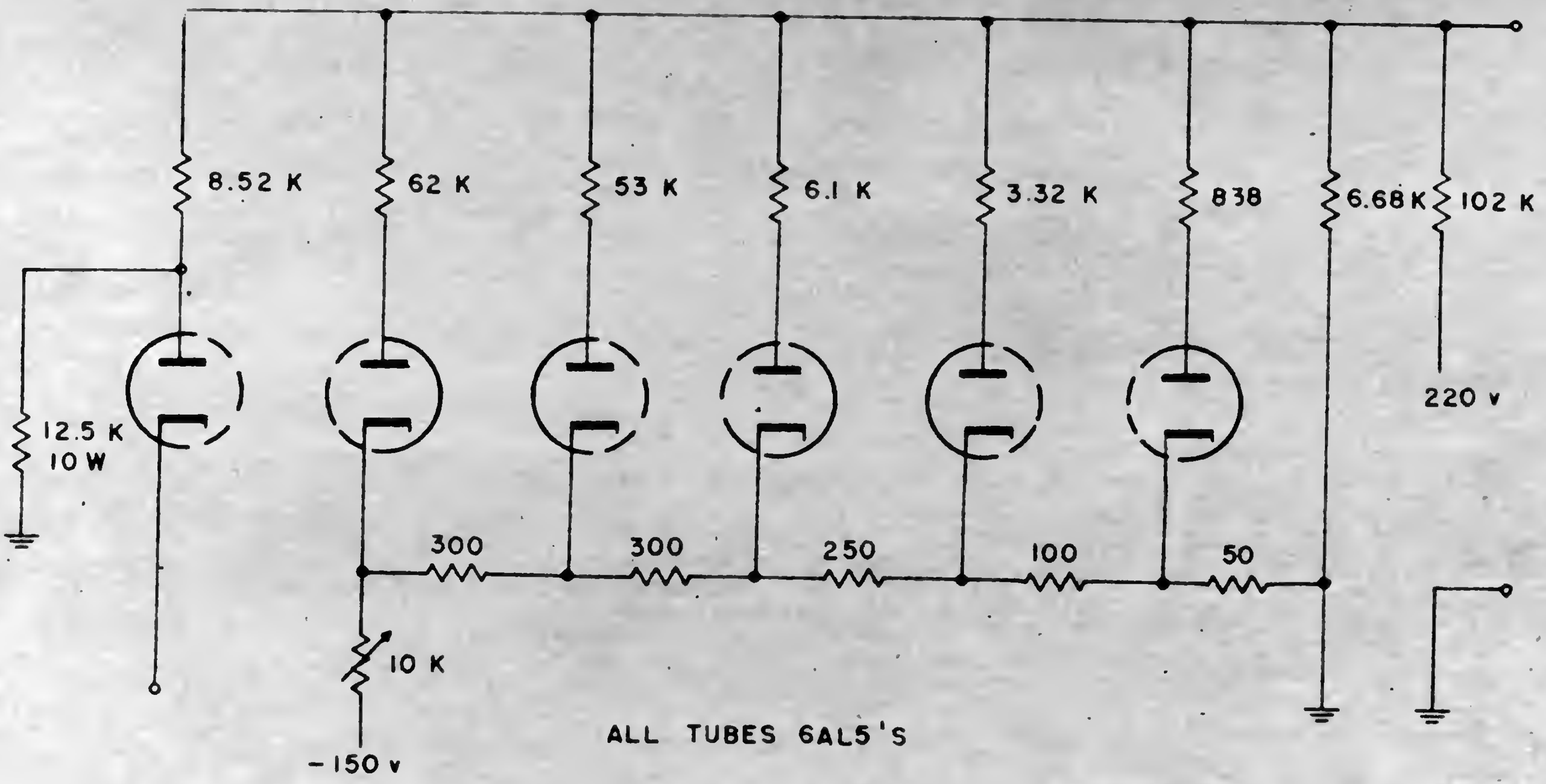

ALL TUBES 6AL5'S

FIG I-3

SQUARE LAW CIRCUIT

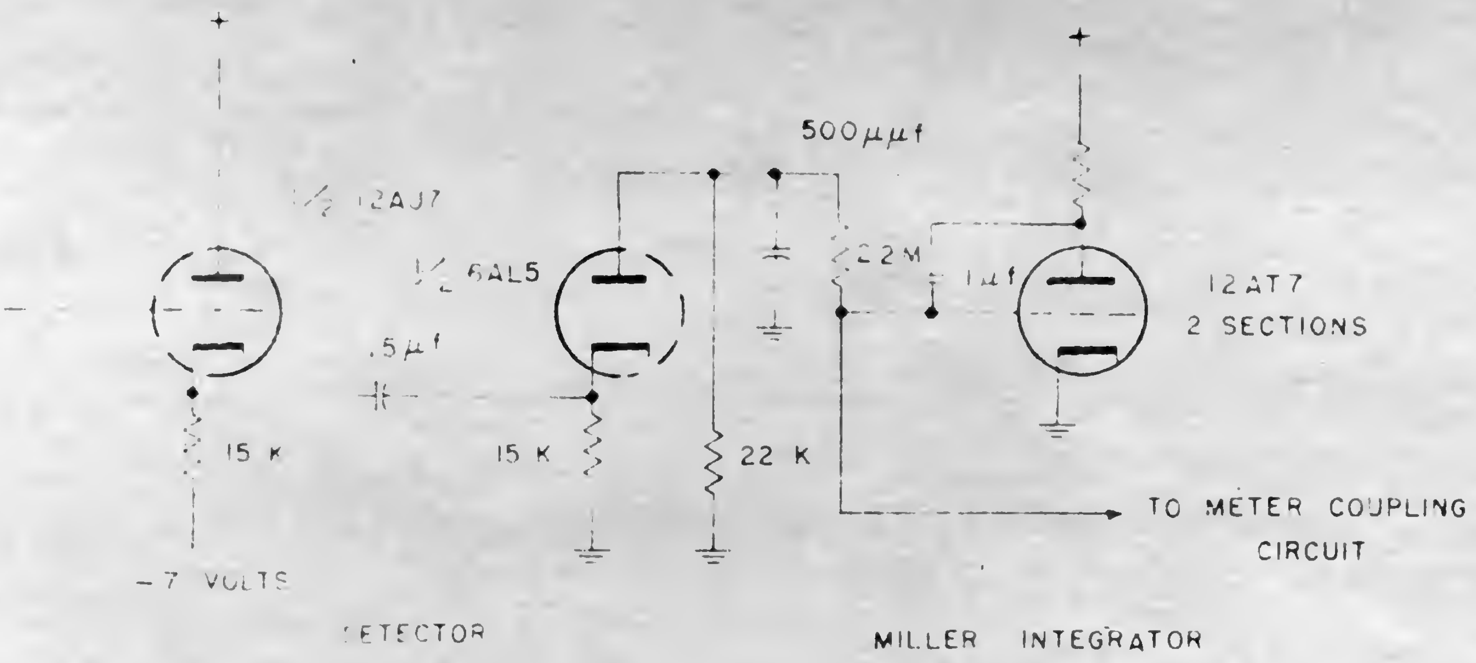

1/2 12AJ7
1/2 6AL5
.5 μf
15 K
15 K
22 K
-7 VOLTS
DETECTOR
500 μμf
2.2 M
1 μf
12AT7
2 SECTIONS
TO METER COUPLING
CIRCUIT
MILLER INTEGRATOR

FIG I-4

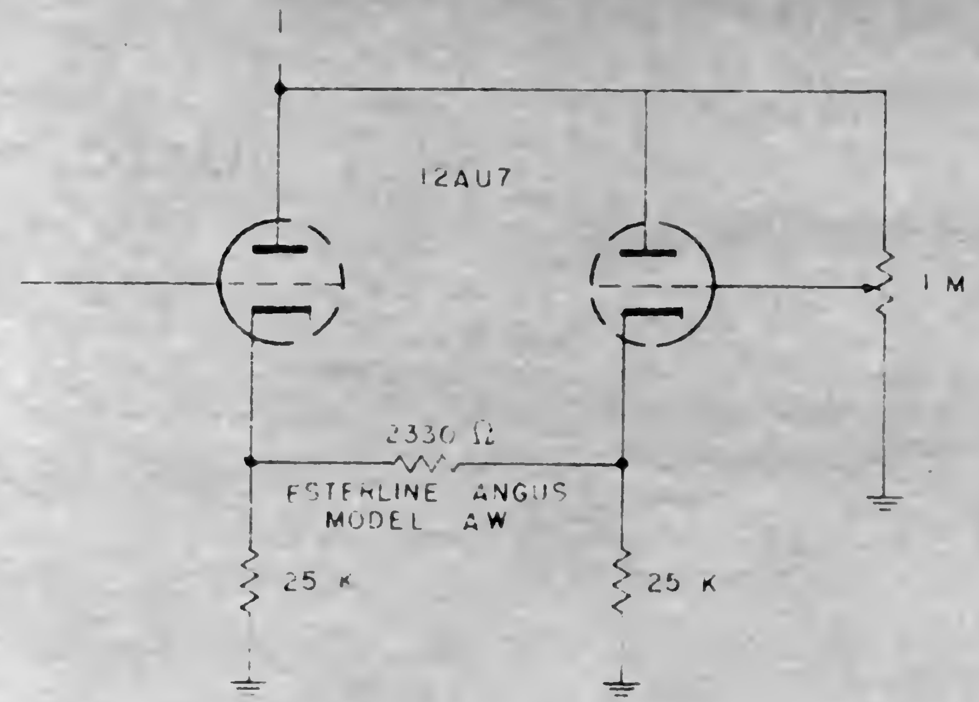

FIG I-5

METER COUPLING CIRCUIT

2. System II - NAVIGATIONAL DEVICE SIMULATOR & RECORDER

As was previously stated, this system must duplicate a navigational device that is represented by the diagram in Figure 1. It must record noise voltage but must disregard the signal, so that if the circuit shown in Figure 1 were used in its entirety, a recording of the output would simply be the average value of the input signal and noise lumped together with no means of distinguishing one from the other. It is required then, that the signal must be eliminated and only the noise voltage recorded. Filtering of course will be useless since it removes those noise frequencies that are of interest, so that the only solution is to phase out the signal. This will require two separate channels and the use of phase shifters, but in keeping with the basic premise, to duplicate the navigational system as much as possible, the only change of significance will be the introduction of a balanced modulator. Its purpose is to act as a gate, opening and closing at a set rate, but 90° out of phase with the gate in the other channel. Thus when the two channels are added together, the signal will have been phased out but the noise components will be the sum of all the cosine terms (from one channel) and all of the sine terms (from the other channel).

Description of Circuits in System II

Figure II-0 Block Diagram of System

Figure II-1 Band Pass Filter and Tuned Amplifier - Essentially this circuit is a single tuned, link coupled circuit, acting as a band pass amplifier with bandwidth of 30 kc with a resonant frequency of 126 kc.

Figure II-2 Logarithmic Amplifier - Same as System I.

Figure II-3 126 kc Crystal Oscillator and Phasing Networks. A highly stable Pierce crystal controlled oscillator is used as a local oscillator, the output of which is fed to two RC type phasing networks. If the output of the oscillator is

$$e_o = E \sin w_o t$$

then the outputs of the phasing networks will be respectively

$$e_1 = E \sin w_o t - 45^\circ$$

and

$$e_2 = E \sin w_o t + 45^\circ$$

Since e_1 and e_2 are ninety degrees apart and bear no fixed relationship to the input signal as yet, they can be represented as

$$e_1 = E \sin w_o t$$

$$e_2 = E \cos w_o t$$

Each are amplified in separate channels and remain in these channels until detections take place.

Figure II-4 126 kc Amplifier, Gate and Integrator - The first two stages are voltage gain stages which split e_1 into two voltages 180° apart in phase and thus drive a push pull cathode follower stage. By this means it is possible to offer a low impedance driving source to the balanced modulator (gate).

Frequency Analysis of Coherent Detector (Balanced Modulator)

If the input noise voltage has the form at the output of the log amplifier of

$$e(t) = A_1 (t) \sin wt + A_2 (t) \cos wt$$

where

$$w = 2\pi (126 \text{ kc} \pm 30 \text{ kc})$$

the output of the balanced modulator can be computed in the following manner.

Assuming matched diodes with similar current characteristics, the current can be represented by the infinite series

$$i_p = a_o + a_1 e + a_2 e^2 + a_3 e^3 + \ldots + a_n e^n$$

Since the integrator will act as a low pass filter on the difference terms of the output of the non-linear device will be of consequence. The d-c term (a_o) can be ignored since transformer coupling is used.

The voltage at point (1), Figure II-5 is

$$E_1 = e_1 + e(t)$$

The voltage at point (2), Figure II-5 is

$$E_2 = - e_1 + e(t)$$

thus the value of e_{out} can be written as

$$\frac{e_o}{R} = i_o = a_2 e^2 = A(E_2 - e_o)^2 - A(e_o - E_1)^2$$

Setting AR = 1/K

$$K\ e_o = (-e_1 + e(t) - e_o)^2 - (e_o - e_1 - e(t))^2$$

Thus

$$e_o = \frac{-4\ e_1\ e(t)}{K - 4\ e_1}$$

Substituting

$$e_o = \frac{-4\ E\ A_1(t)\ \sin w_o t\ \sin wt - 4\ E\ A_2(t)\ \sin w_o t\ \cos wt}{K - 4\ E\ \sin w_o t}$$

Since only the difference terms are of consequence

$$- \sin w_o t\ \cos wt = - \sin (w_o - w)\ t - \cos w_o t\ \sin wt$$

and

$$\sin w_o t\ \sin wt = - \cos (w_o - w)\ t + \cos w_o\ \cos wt$$

Thus e_o can be represented as a voltage having frequencies made up of the difference terms.

For channel two the analysis is the same with the exception of the value of e_2

$$e_o = \frac{-4\ e_2\ e(t)}{K - 4\ e_2}$$

Substituting

$$e_o = \frac{-4\ E\ A_1\ (t) \cos w_o t \sin wt - 4\ E\ A_2(t) \cos w_o t \cos wt}{K - 4\ E \cos w_o t}$$

Again only the difference terms are of consequence

$$- \cos w_o t \sin wt = \sin (w_o - w)t - \sin w_o t \cos wt$$

and

$$- \cos w_o t \cos wt = \sin w_o t \ \sin wt - \cos (w_o - w)\ t$$

as before, the voltage applied to the integrator can be represented as having frequencies made up of the difference terms.

The Miller integrator is similar to that used in System I except that the output can be either a positive or negative value, since the average will vary about zero and will have a mean average level of zero.

Figure II-5 400 Cycle Oscillator and Amplifiers - The 400 cycle oscillator is a Colpitts type with output fed to the two channels after being amplified and shifted in phase 90° with respect to each other by the two RC type networks. The method is similar to that previously mentioned in connection with the 126 kc oscillator and the shift is in keeping with the previous phase shifts. The purpose is to obtain the sum of the two channels across a transformer. It should be mentioned that the shift to 400 cycles is to enable a power gain to be obtained before taking the sum of the two channels.

Figure II-6 400 Cycle Chopper and Amplification Stages. - The 400 cycle chopper is a Model manufactured by the Bristol Co. of Waterbury, Conn..

The necessary power amplification is provided by a single stage in each channel with the two channels being coupled together using a push-pull amplifier. The output to the detector is the sum of the two channels.

Figure II-7 Detector and Recording Circuit - The detector is a peak reading type with a time constant proportional to the 400 cycle frequency. The Recorder is an Esterline Angus, Model AW, having a 1 ma movement.

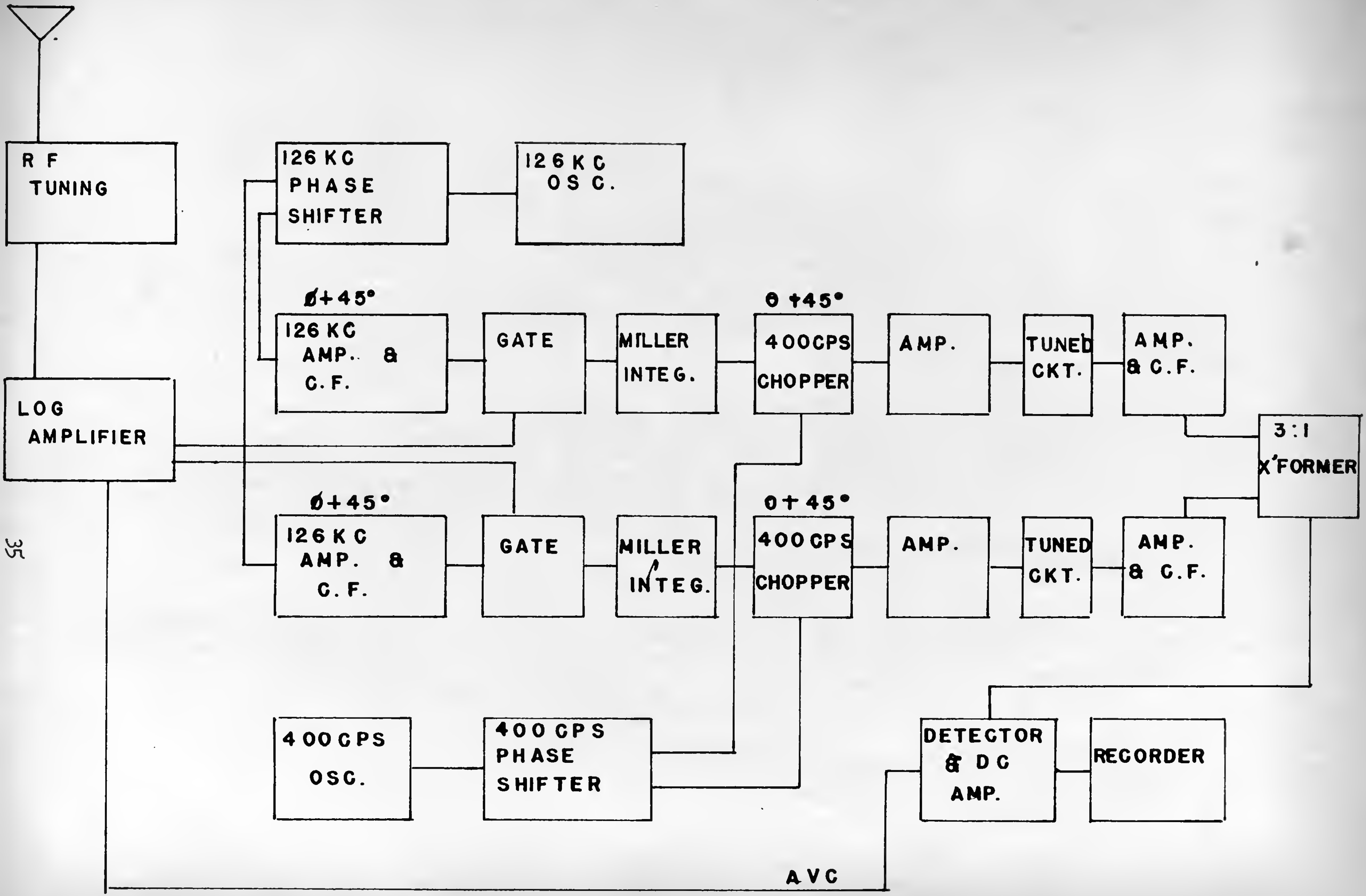
R F TUNING
LOG AMPLIFIER
126 KC PHASE SHIFTER
126 KC OSC.
Ø+45°
126 KC AMP. & C.F.
GATE
MILLER INTEG.
θ +45°
400CPS CHOPPER
AMP.
TUNED CKT.
AMP. & C.F.
3:1 X'FORMER
Ø+45°
126 KC AMP. & C.F.
GATE
MILLER INTEG.
0+45°
400CPS CHOPPER
AMP.
TUNED CKT.
AMP. & C.F.
400 CPS OSC.
400 CPS PHASE SHIFTER
DETECTOR & DC AMP.
RECORDER
AVC

FIG. II-O

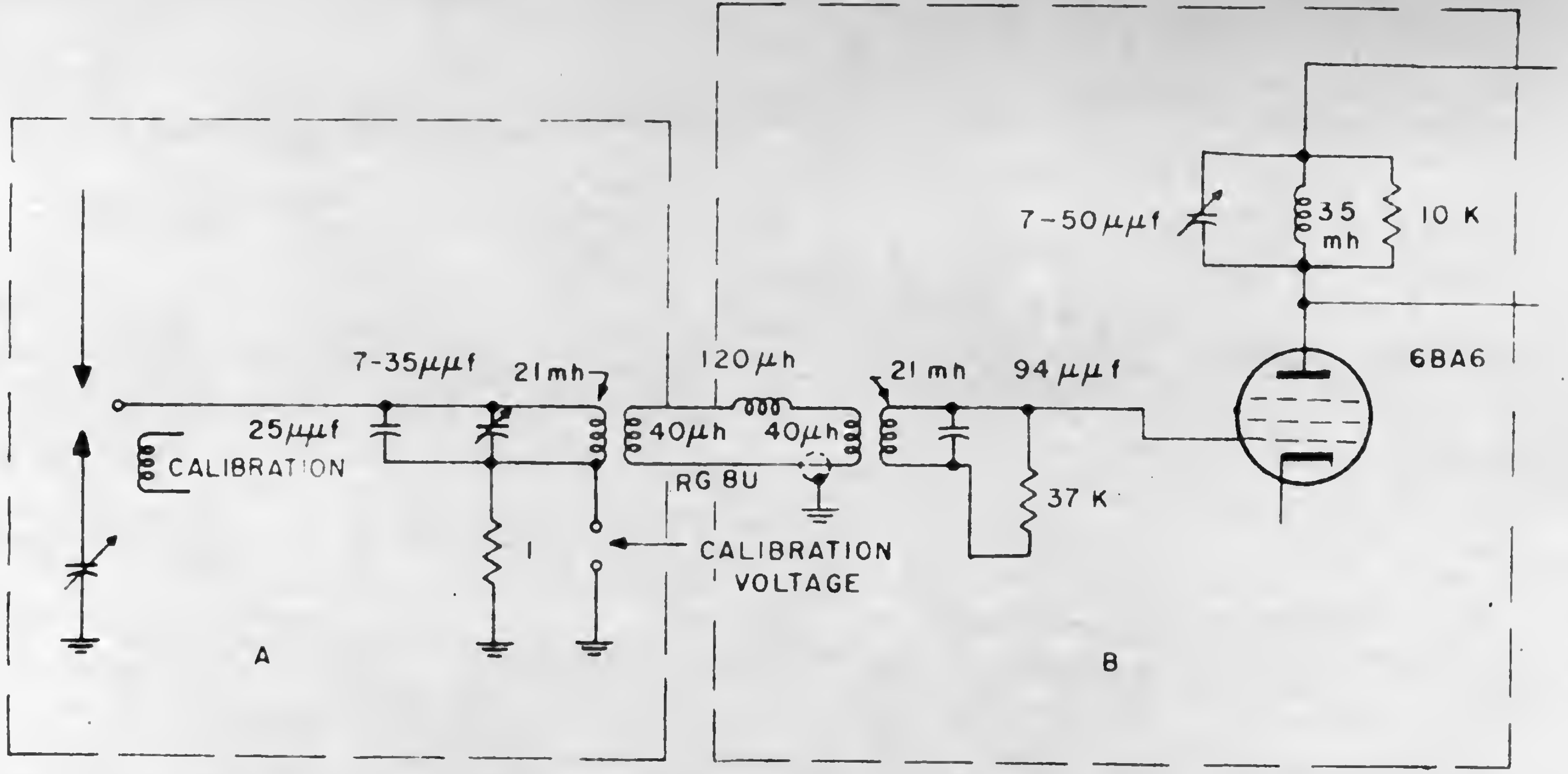

FIG II-1

INPUT CIRCUIT & TUNED AMPLIFIER

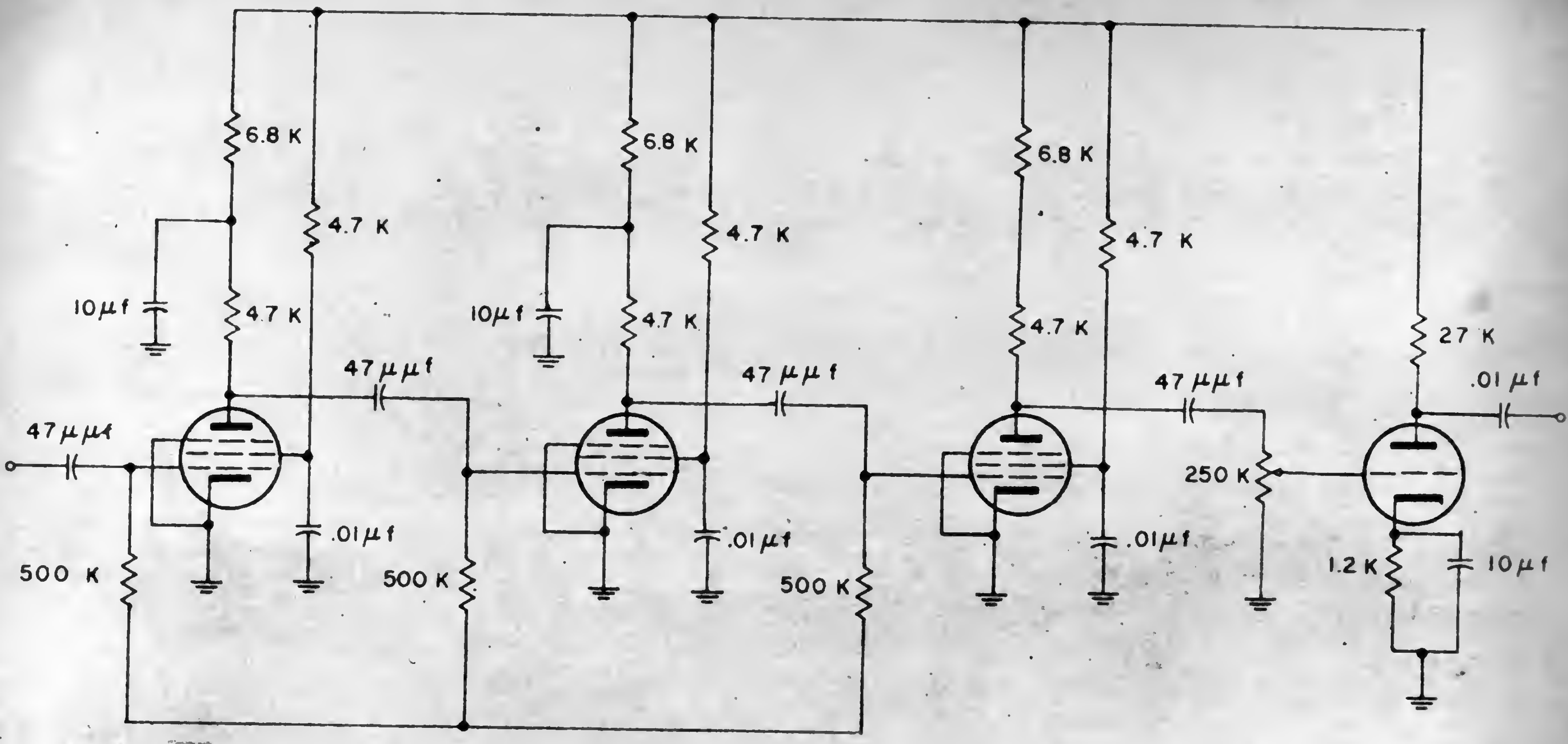

FIG. II-2

LOG AMPLIFIER

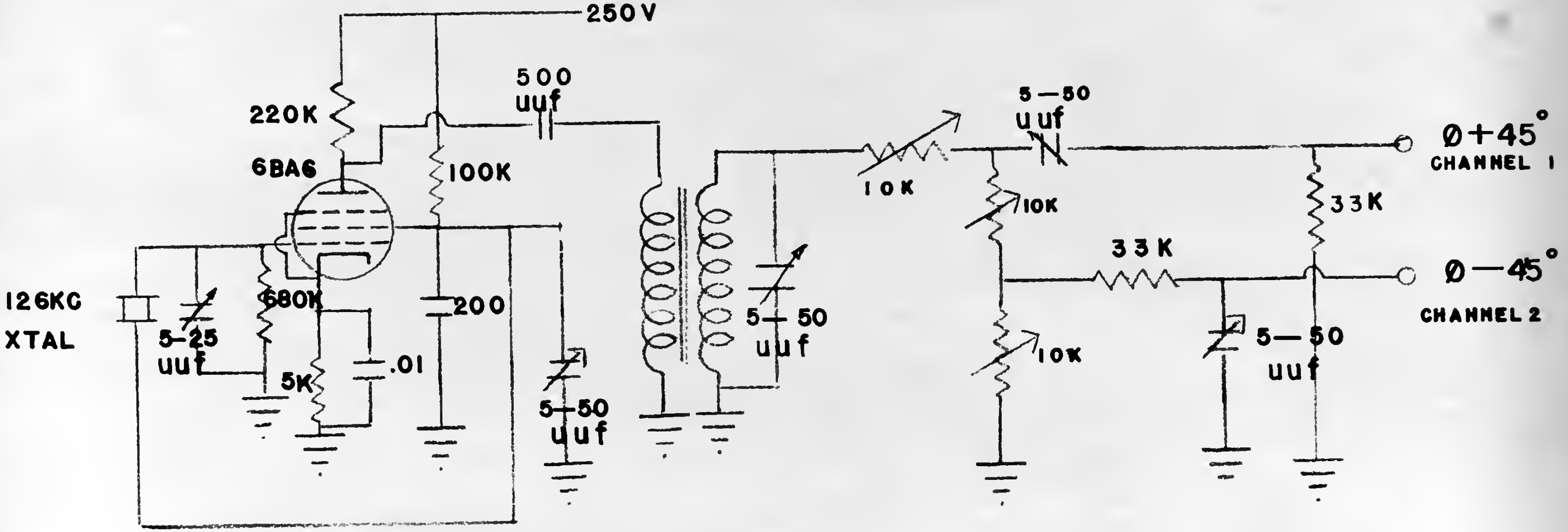

126KC XTAL OSCILLATOR &
PHASE SHIFT NETWORK

FIG. II—3

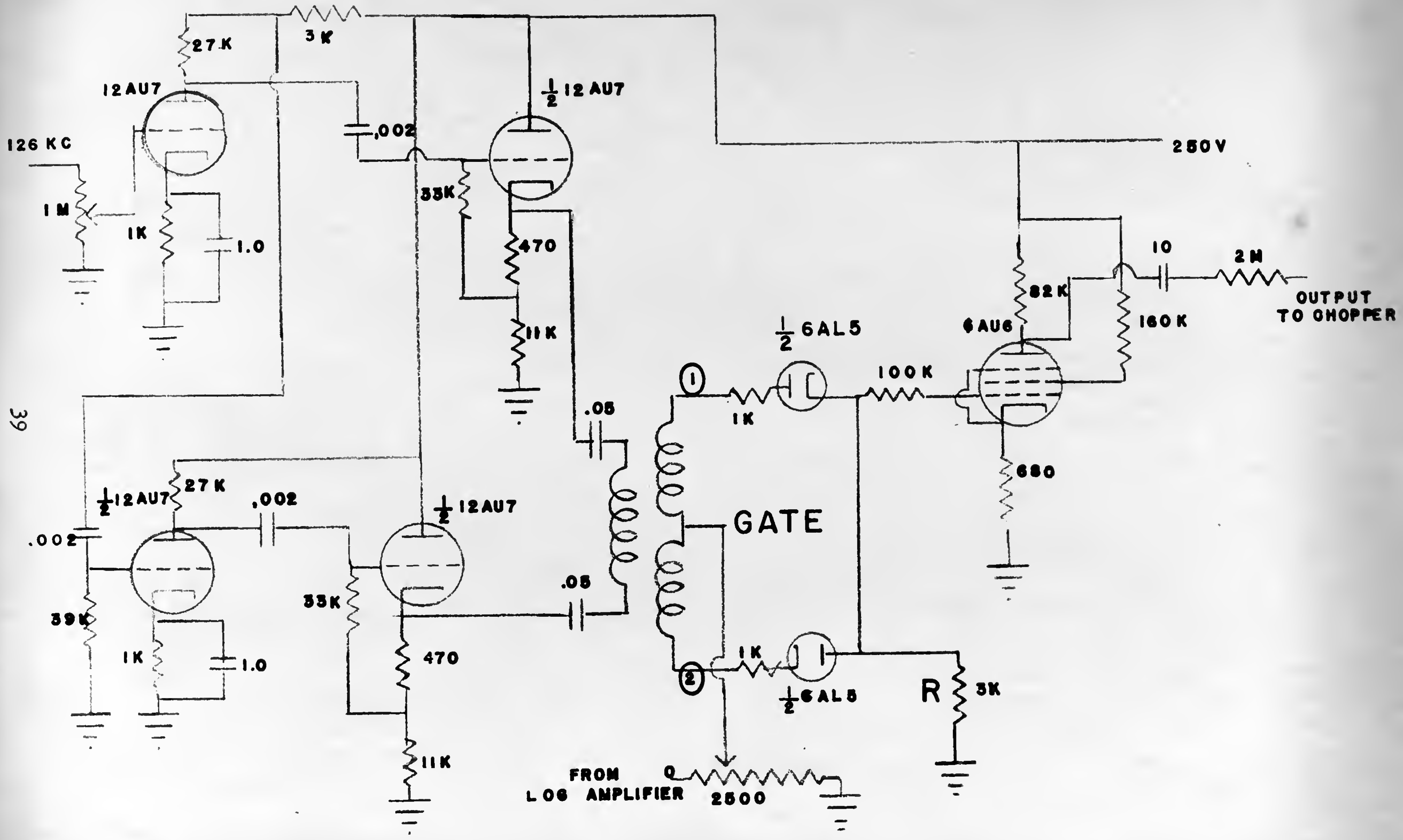

126 KC AMPLIFIER, GATE & MILLER INTEGRATOR

FIG. II — 4

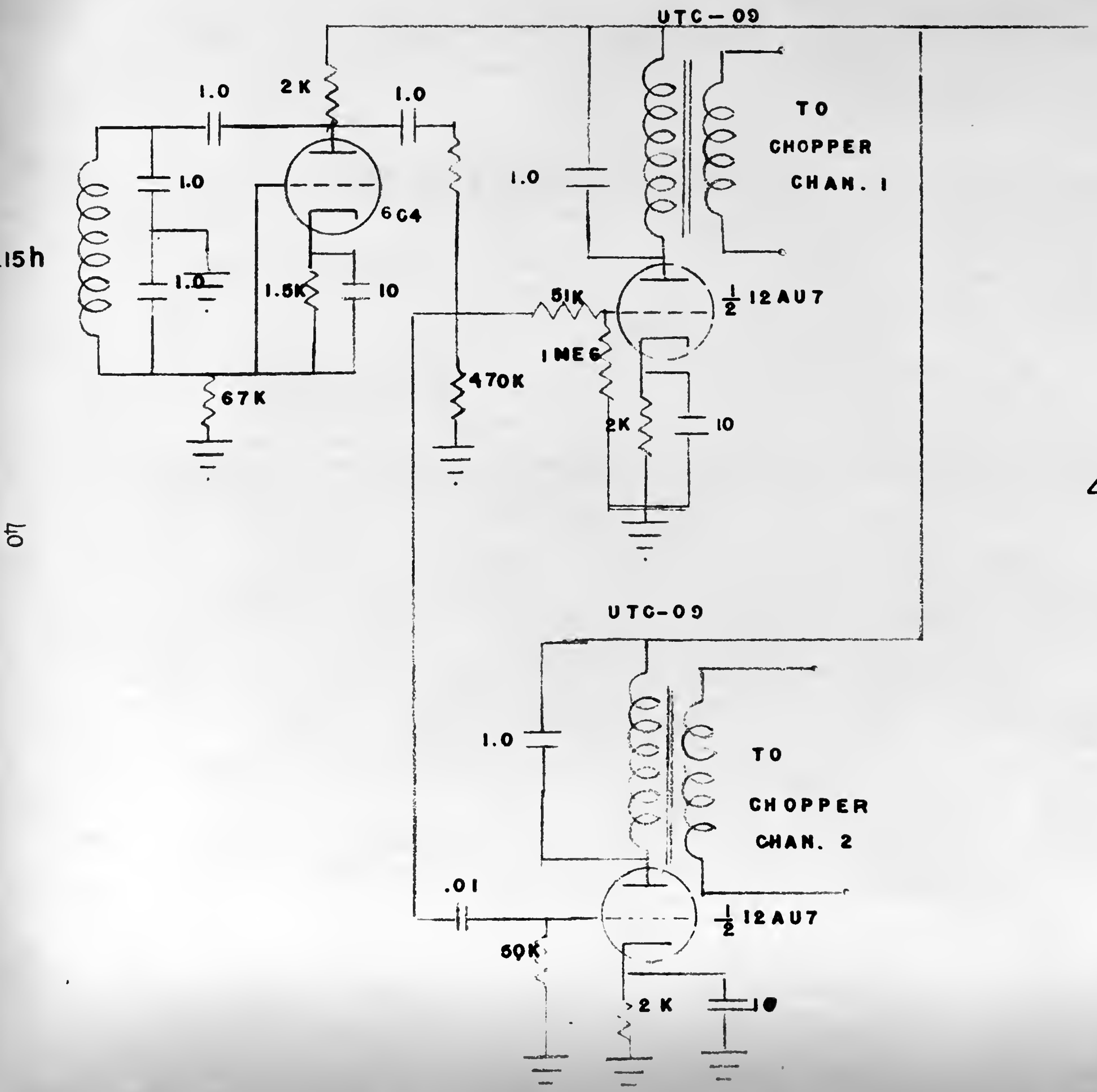

400 CYCLE OSCILLATOR

&

AMPLIFIERS

FIG. II- 5

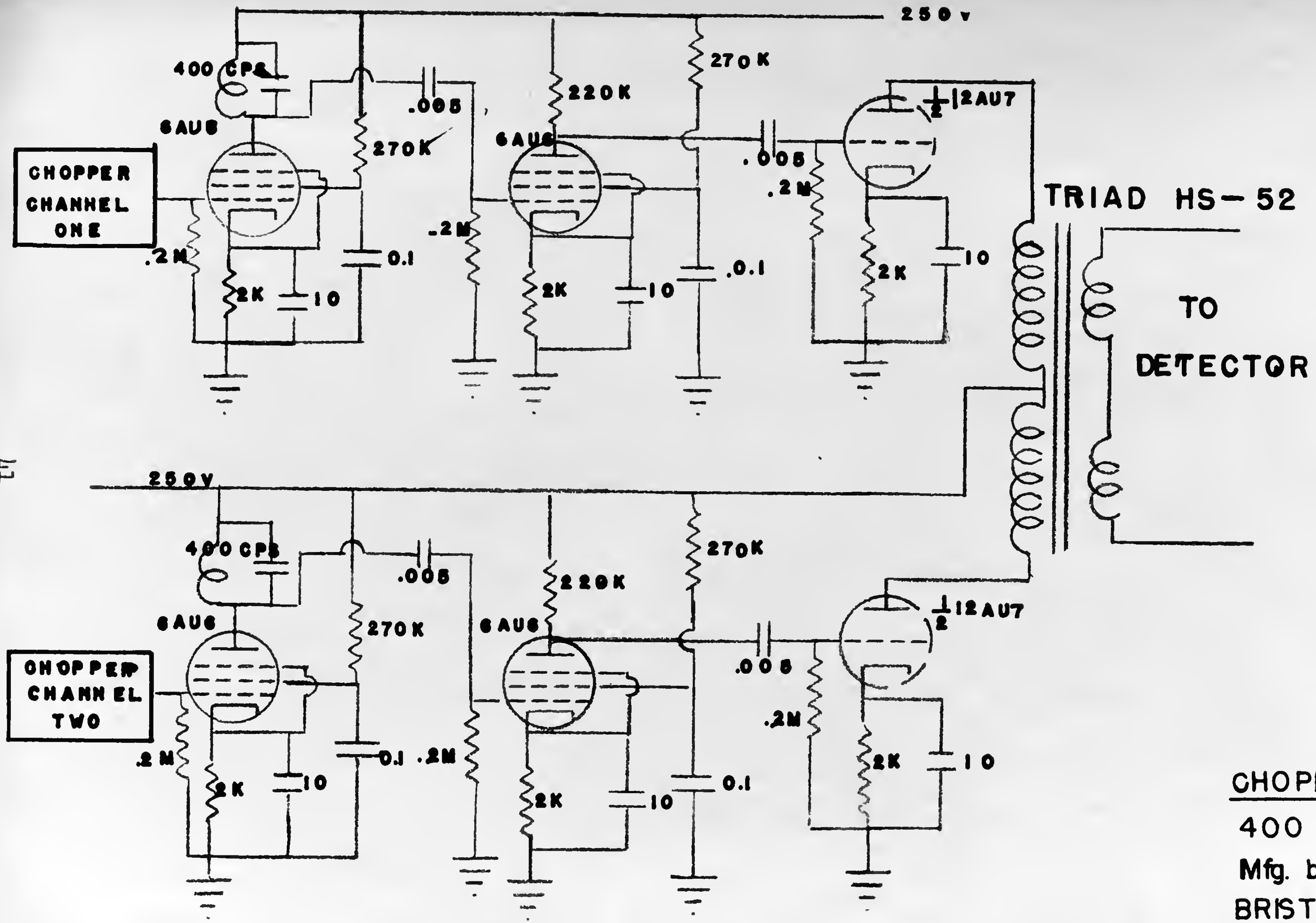

CHOPPER
400 CYCLE
Mfg. by
BRISTOL CO.
WATERBURY, CONN

400 CYCLE CHOPPER & AMPLIFICATION STAGES

FIG. II — 6

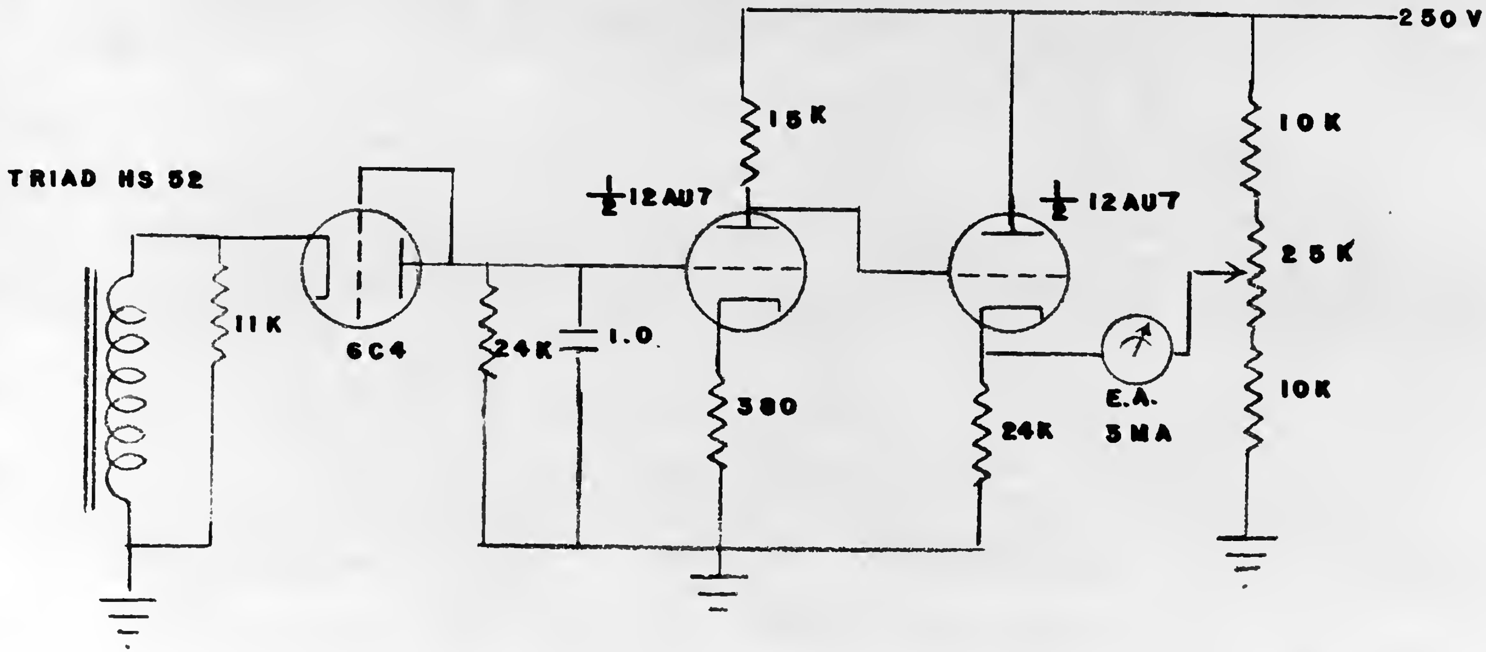

DETECTOR & RECORDER CIRCUIT

FIG. II — 7

3. OPERATION

The technique of taking data is quite simple.

Previous calibration of the meter and circuits should be made in the laboratory using a General Radio Signal Generator 805C, fixed at 126 kc with zero modulation. To simulate an antenna load a value of capacitance equal to the antenna capacitance of the particular aircraft model should be shunted across the input terminals so that the tuning capacitor can be set for the proper value.

For an input of ten microvolts the meter should read a zero value while for a full scale reading a value of 100,000 microvolts can be used. Intermediate points can be located to suit the user.

Flights must be at least four hours long in order to accumulate sufficient data per flight. It has been found that a flight of this duration is necessary mainly to show the magnitude of the error of the navigational device for a known course and speed over a closed geographical loop of known dimensions.

Flights in the vicinity of thunder clouds are desired with a record of the time spent in such locality marked on the recorder paper along side of the measurement record.

CHAPTER III

RESULTS AND CONCLUSIONS

1. Results:

System II was calibrated in the laboratory and will be delivered to the Air Force some time in April 1954. No particular recommendations or conclusions can be offered at this time since no flights have as yet been made, but as is typical with statistical data, the majority of time spent in investigation is used to gather data.

System I was constructed and calibrated in the laboratory during the month of April 1954. A unique testing set up, developed by Tanner[20] was used to generate corona pulses and is illustrated in Figure 5.

Preliminary recordings of the output of this test setup indicated only minute amounts of power were being generated. It was decided to take the unit on a test flight to ascertain whether any general indications of precipitation static could be obtained.

A flight was made on April 14, 1954 from 0830 to 1230 PST with route as follows:

From Monterey, California to Fresno, California, and then north-east to the Sierra Mountain chain, following this due north to Yosemite National Park.

A long line of cumulus type clouds hung over the ridges offering good precipitation static conditions, so the system was placed in operation and immediately the recorder indicated moderate corona because all discharge wicks were removed from the plane previous to take-off. Figures III and IV are parts of the recordings taken during this flight and show vividly

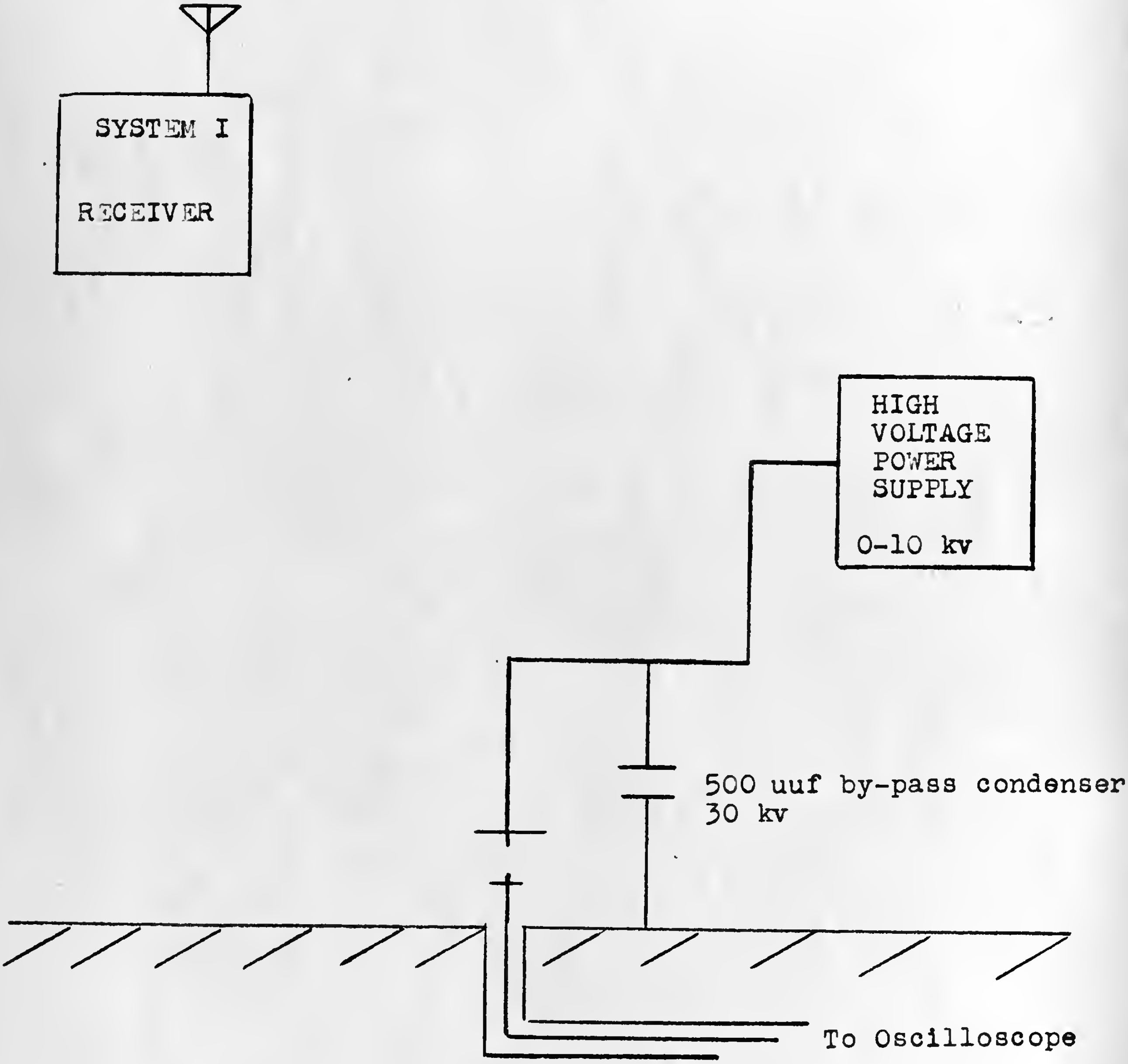

FIGURE 5

Corona Pulse Generator

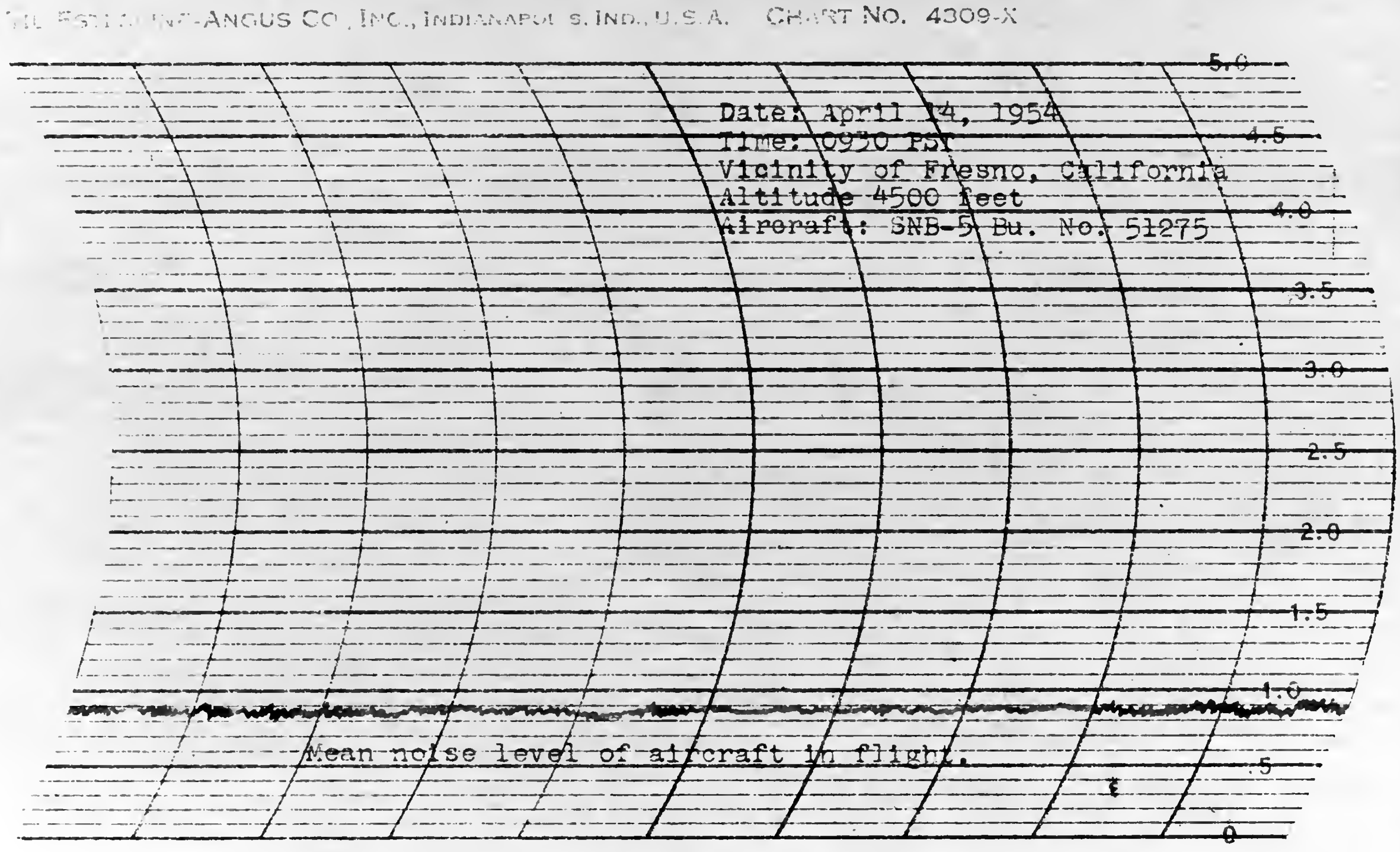

Date: April 14, 1954
Time: 0930 PST
Vicinity of Fresno, California
Altitude 4500 feet
Aircraft: SNB-5 Bu. No. 51275

Mean noise level of aircraft in flight.

FIGURE III

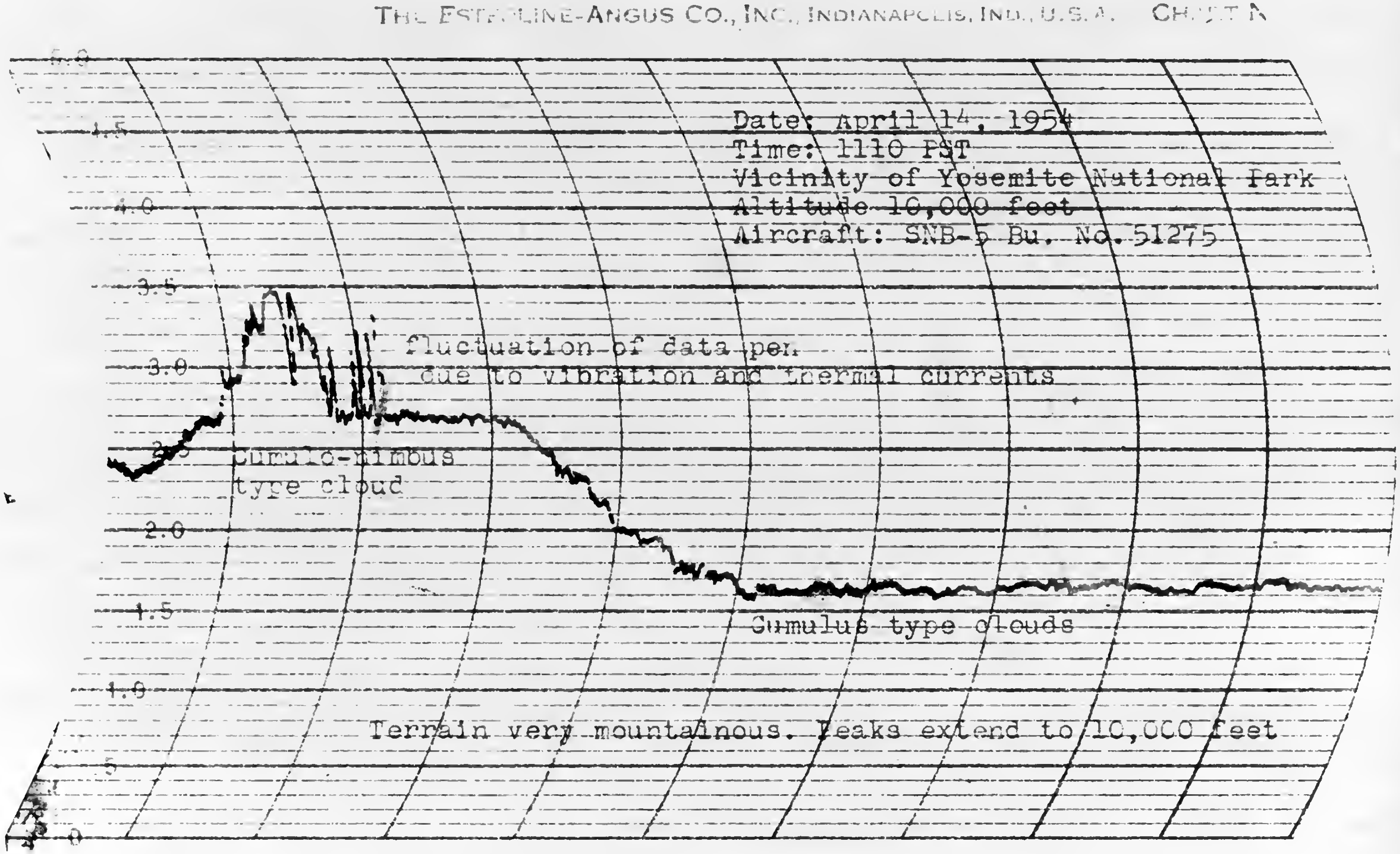

Date: April 14, 1954
Time: 1110 PST
Vicinity of Yosemite National Park
Altitude 10,000 feet
Aircraft: SNB-5 Bu. No. 51275

fluctuation of data pen due to vibration and thermal currents

Cumulo-nimbus type cloud

Cumulus type clouds

Terrain very mountainous. Peaks extend to 10,000 feet

FIGURE IV

the difference in the average power levels for an area of negligible precipitation static and an area of heavy precipitation static.

Conclusions:

Investigations of precipitation static made using System II will record values related only to the average power input to a particular device so it is obvious that this information is of no value to anyone interested in the actual power spectrum or the possible frequency distributions of precipitation static. It was for this purpose that System I was designed.

Since the data gathering period will take considerable time, only a brief outline of the method and approach will be given.

The approach to the problem can be again allied to the familiar treatment of fluctuation noise, using the autocorrelation function and its relation to the Fourier cosine integral.

The autocorrelation function $\phi(\tau)$ of a time function i(t) is defined as the time average of the product of all pairs of points i(t) separated by an interval

$$\phi(\tau) = \lim_{T\to\infty} \frac{1}{2T}\int_{-T}^{T} i(t)\, i(t+\tau)\, dt$$

Substituting from Equation 1-20

$$\phi(\tau) = \nu\int_{-\infty}^{\infty} i(t)\, i(t+\tau)\, dt + \overline{I(t)}^{2}$$

In the above the second term is the square of the d-c value $\overline{I(t)}$.

If a current i(t) is defined as the fluctuation of the current about its mean value, then

$$i(t) = I(t) - \bar{I}$$

$$\phi_i(\tau) = v \int_{-\infty}^{\infty} i(t) \quad i\ (t + \tau)$$

$$\phi_i(0) = \overline{i^2} = v \int_{-\infty}^{\infty} i^2 (t)\ dt$$

Note that the total noise power depends not only upon the average current but on the shape of the current pulse as well.

The noise power spectrum $G_i(w)$ can be obtained from the autocorrelation function by the Fourier cosine integral relation, and is found to be

$$G_i(w) = 2\ v \frac{4\ e}{(w\ \tau_a)^4} (w\ \tau_a)^2\ 2(1 - \cos w \tau_a - w \sin w \tau_a)$$

where e is equal to the charge of electron, and can be plotted as shown in Figure 6.

The noise power in the frequency range f_1 to f_2 is

$$\int_{f_1}^{f_2} G(f)\ df$$

In the frequency range for which $w \tau_a << \pi$, G(f) is nearly constant in value. This is true no matter what the shape of the current pulse is since the value of the Fourier Integral at zero frequency depends only upon the zero moment of the function. Thus G(0) depends only upon the area under $\phi_i\ (\tau)$ and not upon its shape, so that the noise power in a bandwidth Δf is $2\ v\ e \Delta f$.

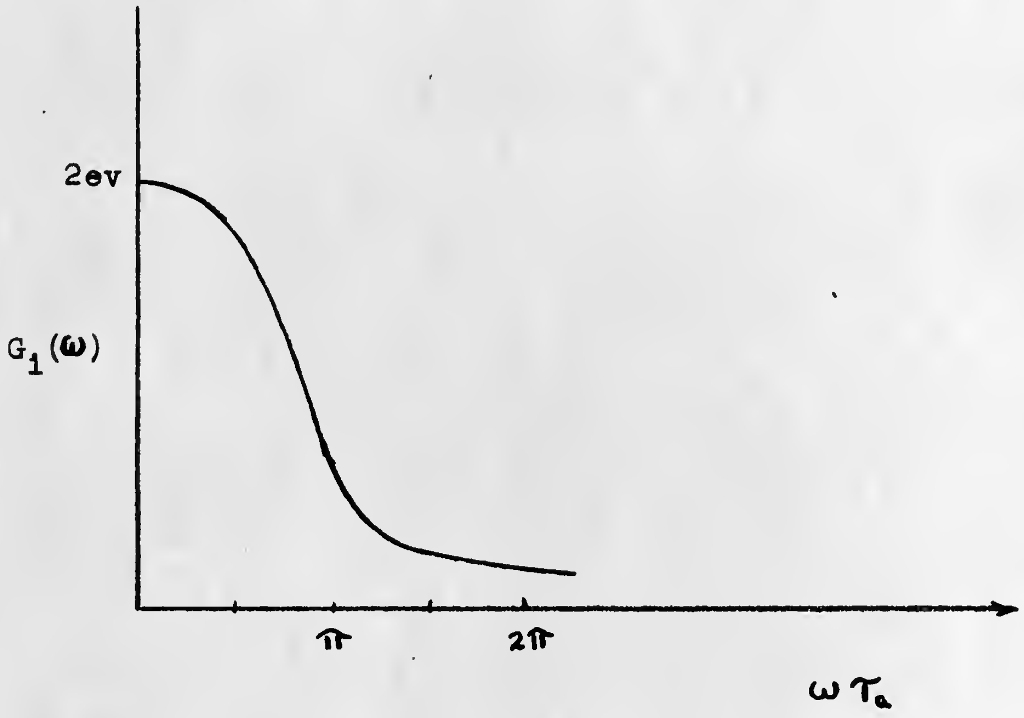

FIGURE 6

Plot of Noise Power Spectrum versus $\omega\tau$

A device then, having a bandwidth that is less than one radian can directly measure increments of the power spectrum. This work is now in progress using System I using the noise model described in the beginning of this chapter. It is obvious that the noise model device is inadequate as a generator for heavy corona conditions and investigation and design of a superior device is contemplated.

APPENDIX I

THE NORMAL DISTRIBUTION

1. Probability:

(a) If an event is certain to occur it is assigned an arbitrary value of unity. For example:

In the toss of a single die the probability of

a six	is	1/6
a five	"	1/6
a four	"	1/6
a three	"	1/6
a two	"	1/6
a one	"	1/6

thus, if six probabilities are mutually exclusive, the probability that either one or the others will occur is equal to the sum of the separate probabilities.

(b) When a particular result in any trial is independent of the results obtained in any other trials, is called a random process. For instance:

A large number of independent trials in tossing a coin might reveal a consecutive string of heads. This will not affect the next toss since the probability is still 1/2 that the coin will come up either a head or a tail.

(c) The probability of the simultaneous occurrence of n events is the product of the n individual probabilities of n events. Thus the probability of winning all tosses in a season of eight footballs games would be $(0.5)^8 = 0.0039$

The above three rules form the basis of the probability distribution laws upon which the mathematical description of noise is based.

2. Distribution formulas:

If the symbol $P_m(n)$ is made to stand for the probability that an event will occur exactly n times in m independent trials, then the basic distribution formula, (Bernoulli Distribution), is

$$P_m(n) = C_n^m \, p^n (1 - p)^{m-n} = \frac{m!}{n!\,(m - n)!} \, p^n (1 - p)^{m-n}$$

where p is the probability for the event to occur in any particular trial.

This specializes to, (Poisson Distribution),

$$P_m(n) = e^{-\bar{n}} \frac{(\bar{n})^n}{n!} \qquad \text{for} \quad \begin{array}{lll} m & \gg & n \\ p & \ll & 1 \\ m & \gg & 1 \end{array}$$

where

$$\bar{n} = mp$$

When n becomes very large as in the case of high density Poisson noise, the above further specializes to the Gaussian Distribution.

$$P_m(n) = \frac{1}{\sqrt{2\pi\bar{n}}} \, e^{-(n-\bar{n})^2/2\bar{n}}$$

when $\quad n \gg 1$

$$\frac{n - \bar{n}}{\bar{n}} \ll 1$$

$$n - \bar{n} \gg 1$$

3. The Central Limit Theorem

The Central Limit Theorem states that subject to very lenient conditions, and regardless of the amplitude distributions of the individual components, as the number of components n approaches infinity, the amplitude distribution of the current approaches the Gaussian or normal distribution.

Thus it is possible to relate the limiting form of the Gaussian Distribution to the Mathematical Description of Noise (ChapterI) by virtue of the large number of independent events (electron crossings) which add up to give the independent variable I. This distribution will be independent of the amplitude distributions of the individual events (shapes of the electron pulses). It is required, generally speaking, that the contributions of the individual components be small compared with the total value of the sum

APPENDIX II

PROPERTIES OF NARROW BAND NOISE

1. Examining the statistical properties of the output of a narrow band filter plotted in Figure A-I, and the assumption, that the band width of the filter, $f_m << f_o$, the output can be expressed in the form

$$e(t) = E(t) \cos (w_m t + \phi(t)) \qquad \text{II-1}$$

provided that the input noise has a Gaussian distribution.

E(t) then represents the magnitude of the envelope of the output and $\phi(t)$ the phases changes.

Using the Fourier representation of the output as

$$e(t) = \sum (a_n \cos nw_o t + b_n \sin nw_o t) \qquad \text{II-2}$$

where the summation is to include all frequencies which is in the range of the filter.

Setting up the sum and difference terms so as to show relationship to a sine wave of frequency w_m:

$$\cos nw_o t = \cos \left[(nw_o - w_m)t + w_m t \right] \qquad \text{II-3}$$

$$= \cos (nw_o - w_m)t \cos w_m t - \sin (nw_o - w_m) \sin w_m t$$

$$\sin nw_o t = \sin \left[(nw_o - w_m)t + w_m t \right] \qquad \text{II-4}$$

$$= \sin (nw_o - w_m)t \cos w_m t + \cos (nw_o - w_m)t \sin w_m t$$

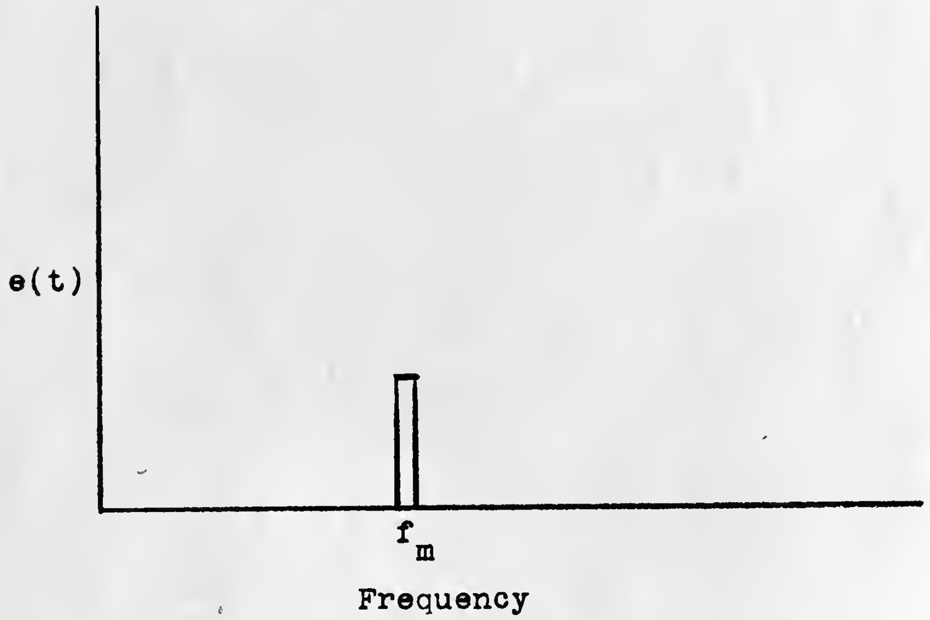

FIGURE A-I

Output of a Narrow Band Filter

Letting $e_{cos}(t)$ represent the summation of all the coefficients of $\cos w_m t$ in the expression for $e(t)$, and $e_{sin}(t)$ represent the summation of the coefficients of $\sin w_m t$, then

$$e_{cos}(t) \overset{\Delta}{=} \sum_n \left[a_n \cos (nw_o - w_m)t + b_n \sin (nw_o - w_m)t \right] \qquad \text{II-5}$$

and

$$e_{sin}(t) \overset{\Delta}{=} \sum_n \left[b_n \cos (nw_o - w_m)t - a_n \sin (nw_o - w_m)t \right] \qquad \text{II-6}$$

Substituting

$$e(t) = e_{cos}(t) \cos w_m t + e_{sin}(t) \sin w_m t \qquad \text{II-7}$$

Thus, $e_{cos}(t)$ and $e_{sin}(t)$, are slowly varying compared with $\cos w_m t$ or $\sin w_m t$.

From the Expression III-1, the magnitude

$$E(t) = \sqrt{e^2_{cos}(t) + e^2_{sin}(t)} \qquad \text{II-8}$$

and

$$\phi(t) = \tan^{-1} -e_{sin}(t) / e_{cos}(t) \qquad \text{II-9}$$

The random variables $e_{cos}(t)$ and $e_{sin}(t)$ are sums of independent variables with Gaussian amplitude distributions. The average power can then be written as

$$\frac{\overline{E^2}}{2} = \frac{\overline{e^2_{\cos}}}{2} \qquad \frac{\overline{e^2_{\sin}}}{2} = \overline{e^2} \tag{II-10}$$

where

$$e^2_{\cos} = \sum_n a_n^2$$

and

$$e^2_{\sin} = \sum_n b_n^2$$

BIBLIOGRAPHY

1. Bennett, R. R. and Fulton, A. S., "The Generation and Measurement of Low Frequency Random Noise", J. A. P., Vol. 22, No. 9, September 1951.

2. Blanchard, H. P. and Lynch, W. M., "Monthly Report of Low Frequency Loran Research", Report No. 29 on Contract No. W 28-099 ac157, Watson Laboratories, Cambridge, Mass.

3. Cramer, H., "Mathematical Methods of Statistics", Princeton University Press, Princeton, N. J., 1947.

4. Davenport, W. B., Jr., and R. A. Johnson and D. Middleton, "Statistical Errors in Measurements on Random Time Functions", J. A. P., Vol. 23, No. 4, April 1952.

5. George, T. S., "Report on Statistical Theory of Noise", Copy No. 231, Report No. 102, Philco Research Division, Philadelphia, 1947.

6. Goldman, S., "Frequency Analysis, Modulation and Noise" pp. 288-351, McGraw-Hill Book Co., Inc., New York, 1948.

7. Goldman, S., "Information Theory", pp. 85-123, Prentice-Hall Inc., New York, 1953.

8. Gunn, Ross, et al, "Army-Navy Precipitation Static Project", Proc. IRE Vol. 34, Nos. 4 and 5, April-May 1946.
    - Pt. I The Precipitation-static interference problem and methods for its investigation.
    - Pt. II Aircraft Instrumentation for precipitation static research.
    - Pt. III Electrification of aircraft flying in precipitation areas.
    - Pt. IV Investigation of methods for reducing precipitation static radio interference.
    - Pt. V The high voltage characteristics of aircraft in flight.
    - Pt. VI High voltage installation of the precipitation static project.

9. Harmon, W. W., "EE-251, Course Notes on Noise Analysis", Stanford University Electrical Engineering Department, Stanford, California, 1953.

10. Hoff, R. S. and Johnson, R. C., "A Statistical Approach to the Measurement of Atmospheric Noise", Proc. IRE, Vol. 40, No. 2, February, 1952.

11. Hucke, Herbert M., "Precipitation Static Interference", Proc IRE, Vol. 27, No. 5, May 1939.

BIBLIOGRAPHY

12. Knudzton, N., "Experimental Study of Statistical Characteristics of Filtered Random Noise", Tech. Report No. 115, on Contract No. W36-039-sc-32037, Research Laboratory of Electronics, MIT, Cambridge, Mass. 1949.

13. Landon, V. D., "The Distribution of Amplitude with Time in Fluctuation Noise", Proc. IRE, Vol. 29, No. 2. February 1941.

14. Landon, V. D., and Norton, K. A., "Discussion on the Distribution of Amplitude with Time in Fluctuation Noise", Proc. IRE, Vol. 30, No. 9, September 1942.

15. Lawson, J. L. and Uhlenbeck, G. E., "Threshold Signals", pp 3-47, McGraw-Hill Book Co. Inc., New York 1950.

16. Lee, Y. W. and Stutt, C. A., "Statistical Prediction of Noise", Tech. Report No. 129 on Contract No. W36-039-sc32037, Research Laboratory of Electronics, MIT, Cambridge, Mass. 1949.

17. Middleton, D., "On the Theory of Random Noise, Phenomenological Models", J. A. P., Vol. 22, No. 9, September 1951.

18. Rayleigh, Lord, "The Theory of Sound", Macmillan and Co., London, 1926.

19. Rice, S. O., "Mathematical Analysis of Random Noise", B. S. T. J., July 1944, No. 23, pp. 282-332, No. 24, pp. 46-156, January 1945.

20. Tanner, R. L., "Radio Interference from Corona Discharges", Technical Report No. 37, Stanford Research Project No. 591, Air Force Contract No. AF 19(604)-266, April 1953.

21. Wiener, N., "Cybernetics", Chapter III, John Wiley and Sons, Inc., New York, 1949.

22. Wiener, N., "The Extrapolation, Interpolation, and Smoothing of Stationary Time Series", John Wiley and Sons, New York, 1949.

23. Woodward, P. M., "Probability and Information Theory with Applications to Radar", McGraw-Hill Book Co., Inc., New York, 1953.